1 2 9 0

UNIVERSIDADE DE
COIMBRA

Edona Hyla

INFLUENCE OF SOOT ON TRIBOLOGICAL PERFORMANCE OF UNCOATED AND DLC-COATED LUBRICATED CONTACTS

FRICTION AND WEAR ANALYSIS

VOLUME 1

Dissertação no âmbito do Mestrado Conjunto Europeu em Tribologia de Superfícies e Interfaces orientada pelo Professor Doutor AlbanoAugusto Cavaleiro Rodrigues de Carvalho apresentada ao Departamento de Engenharia Mecânica da Faculdade de Ciências e Tecnologia da Universidade de Coimbra

Julho de 2019

FCTUC FACULDADE DE CIÊNCIAS
E TECNOLOGIA
UNIVERSIDADE DE COIMBRA

DEPARTAMENTO DE ENGENHARIA MECÂNICA

Influence of soot on tribological performance of uncoated and DLC-coated lubricated contacts

Friction and wear analysis

Submitted in Partial Fulfilment of the Requirements for the Degree of Master in Tribology of Surface and Interfaces

Author
Edona Hyla

Advisor
Professor Albano Cavaleiro

Jury

President **Professor Doctor Bruno Trindade**
Professor at University of Coimbra

Vowels **Professor Doctor Albano Cavaleiro**
Professor at University of Coimbra
Doctor João Paulo Dias
Adjunct Director of Instituto Pedro Nunes (IPN)

In the framework of Joint European Master in Tribology of Surfaces and Interfaces

tribos
joint european master
in tribology
of surfaces and interf
Ljubljana • Leeds • Coimbra • Luleå

Coimbra, July 2019

Dedication

Dedicated to my grandfathers, Fehmi Hyla and Hasan Perolli, who taught me that kindness and a pure heart exceeds the value of each treasure in this world.
To their inspiration, love and lessons, which will live as long as I do.

Dedikim

Dedikuar gjyshërve të mi, Fehmi Hyla dhe Hasan Perolli, të cilët më mësuan se mirësia dhe zemra e pastër e tejkalonjnë vlerën e çdo thesari në këtë botë.
Për frymëzimin e tyre, dashurinë dhe mësimet, të cilat do të jetojnë për aq kohë sa unë do jem gjallë.

Acknowledgment

First and foremost, I want to thank my supervisor Prof. Dr. Albano Cavaleiro for his support and professional assistance throughout all the time. I want to mention the fact that he was always available and helpful when I run into a problem or had any questions. I would like to thank you very much for your patience and understanding during the past year.

I am very grateful to every each of our TRIBOS coordinators, Prof. Dr. Ardian Morina (University of Leeds), Prof. Dr. Mitjan Kalin (University of Ljubljana), Prof. Bruno Trindade (University of Coimbra) and Prof. Dr. Nazanin Emami (Lulea University of Technology), for their unconditioned help, guidance and impact on my personal growth. Because of your hard work and your passion, I am now able to proceed with mine.

To continue this research in March 2019, I went to Ducom Instruments Europe B.V., located in Netherlands. My time there was an extraordinary experience. I would like to thank Deepak H. Veeregowda for always being inspiring, expand my horizon and enriching me as a researcher. I must also thank Angel Maria Tortora and Fabio Alemanno who kindly assisted me during my entire stay.

Getting though this program required more than academic support, I can consider myself very lucky to have plenty of it from people I can call my friends. To my old ones who I can always go back home and to the new ones opening their heart and homes to me, thank you! With a special mention to Muhamad Yousri and Yasmin Hayatgheib. I will never forget the long nights and walks when you have been supporters, listeners and teachers for me. By expressing my gratitude and appreciation for your friendship I would exceed this thesis page limit. Thank you!

To my father Lulzim Hyla, my mother Hermelinda Hyla, my sisters Hira and Xhentila Hyla and my whole family, thank you for offering me your encouragement and motivation every day, for believing in me when I did not believe in myself and for getting me up whenever I felt down, nothing of this would have been possible without you. This thesis will forever stand as a testament to your unconditional love.

Abstract

This project is motivated from now days trends in the automotive industry to increase fuel efficiency and fulfill environmental standards. To do so the increase of soot (carbon black particles) in the Internal Combustion Engines has become a big issue, challenging the environmental impact of disposing oil and overall maintenance cost of running a vehicle.

Diamond Like Carbon (DLC) thin films are widely used for protection of components under high load from wear and/to reduce friction loses in combustion engines. To furthermore increase the properties of DLC, in this study DLC doped with tungsten (W-DLC) and DLC doped with silver (Ag-DLC) have been used.

In basic, the interaction among soot and steel surfaces that are coated with W-DLC and Ag-DLC thin film as a possible solution to the soot wear problems and further development of soot wear resistant lubricants has been investigated.

Friction and wear properties of W-DLC and Ag-DLC have been tested in boundary lubrication conditions using a 4 Ball Test, for post analyses Optical Microscope, 3D Profilometry and Raman Spectroscopy have been applied.

Table of contents

1. Introduction 1
  1.1 Automotive Industries 1
  1.2 What is Tribology? 1
  1.3 Introduction to Friction 1
  1.4 Introduction to Wear 2
  1.5 How is the engine affected by Tribology? 2
  1.6 Motives for tribological design and innovation 3
  1.7 What is soot and why is it a mayor issue for the automotive industry 3
2. Aim and Objective 6
3. State of Art 7
  3.1 Automotive engine, friction and wear reduction trends 7
  3.2 Lubricants and Lubrication 8
  3.3 Base oil 9
    3.3.1Ester based oil 9
  3.4 Additives 10
    3.4.1Glycerol Monooleate 10
  3.5 Carbon Black Soot Particles in Engine Oil 11
  3.6 Theories about soot wear 12
  3.7 Materials 14
    3.7.1 DLC 14
    3.7.2 W-DLC 14
    3.7.3 Ag-DLC 15
4. Experimental details and characterizations 16
  4.1 Tribological Testing 16
    4.1.1 Equipment set-up and test parameters 16
    4.1.2 Materials and preparatory procedures applied 17
  4.2 Coatings 18
  4.2.1 DC Magnetron Sputtering 18
    4.2.2 Ag-DLC Coating Deposition 19
    4.2.3 W-DLC Coating Deposition 20
    4.2.4 Ag-DLC coating characterization 21
    4.2.5 W-DLC coating characterization 23
4.3 Post test analyses 24
    4.3.1 Optical Microscopy 24
    4.3.2 3D Profilometry 24
    4.3.3 Raman Spectroscopy 25
5. Results 26
  5.1 Tribo-pair set up 26

5.2 W-DLC 28

5.2.1 Friction evaluation.. 28

5.2.2 Wear results... 29

5.2.3 Raman Results 30

5.3 Ag-DLC 37

5.3.1 Friction evaluation.. 37

5.3.2 Wear Results 37

5.3.3 Raman results.. 37

6. Conclusion... 39

7. Future Oil Analyses.. 40

References 41

Annex A – Base Oil and Additive Specifications.. I

Annex B-Coefficient of friction for Steel/W-DLC contact lubricated in the formulated lubricants II

Annex C –Coefficient of friction and mean wear scar diameter for Steel/Ag-DLC contact lubricated in all formulated lubricants III

Annex D – Wear images, Raman spectroscopy and 3D profile of Ag-DLC Wear Scars V

List of Figures

Figure 1.1 Schematic representation of friction force 2

Figure 1.2 STEM micrograph of carbon black particles..4

Figure 3.1 Visible black smoke produced by old vehicles...8

Figure 3.2 API base oil categories..9

Figure 3.3 Schematic representation of working GMO...10

Figure 3. 4 Images of component reciprocating tests performed at 100°C [22]..................13

Figure 4.1 4 ball tester working environment..16

Figure 4.2 Schematic representation of the 4 ball collet set up...16

Figure 4. 3 Schematic representation of DC Magnetron Sputtering.................................19

Figure 4.4 Scanning Electron Microscope (SEM) images of the thickness and cross section morphology of Ag – DLC..21

Figure 4.5 Scratch test of Ag-DLC with the identification of the zones of cohesive failures (yellow) and adhesive failures (orange and red) being the red one indicative of the delamination zone of the coating from the substrate...22

Figure 4.6 SEM images of the thickness and cross section morphology of W–DLC...........23

Figure 4.7 Scratch test on W-DLC with the identification of the zones of cohesive failures (yellow) and adhesive failures (orange and red) being the red one indicative of the delamination zone of the coating from the substrate...23

Figure 4.8 Schematic of an Interferometric profilometer[35]...24

Figure 4.9 Schematic representation of Raman Spectroscopy work flow..........................25

Figure 5.1 Coefficient of friction from 3 different tribo-pair set ups lubricated in base oil..26

Figure 1.2 Mean Wear Scar Diameter from 3 different tribo-pair set ups...........................27

Figure 5.3 Optical image of the wear scar from the upper steel ball in the steel-WDLC set up lubricated in base oil..27

Figure 5.4 3D profile of the wear scar from the upper steel ball in the steel-WDLC set up lubricated in base oil..27

Figure 5.5 Coefficient of friction obtained from the 4 ball tester for steel and W-DLC tribopair lubricated in base oil, base oil containing 1% GMO, base oil containing 1% of soot and base oIl containing 1% GMO and 1% soot...28

Figure 5.6 Coefficient of friction obtained from the 4 ball tester for steel on steel and steel on W-DLC tribopair lubricated in base oil...29

Figure 5.7 Mean wear scar diameter obtained with an optical microscope and measured with AMScope software for steel on steel and steel on WDLC tribopair lubricated in all formulated oils....29

Figure 5.8. Raman Spectra taken inside the wear scar of the steel ball, after the 4 ball test for the steel on steel tribopair lubricated with all formulated lubricants....30

Figure 5.9. Wear scar images and measurements on steel balls obtained with an Optical Microscope fot the steel on steel tribopair lubricated in all formulated lubricants....31

Figure 5.10. a) Wear scar image and dimensions on W-DLC coated steel ball lubricated in base oil. b) Relevant Raman Spectra taken in specified points on the wear scar image. The black spectra belonging to WDLC coating taken outside of the wear scar, it is used as a reference. 32

Figure 5.11. 3D profile of the wear scar on W-DLC coated steel ball lubricated in base oil....32

Figure 5.12 a) Wear scar image and dimensions on W-DLC coated steel ball lubricated in base oil + GMO b) Relevant Raman spectra taken in specified points on the wear scar image....33

Figure 5.13 3D profile of the wear scar on W-DLC coated steel ball lubricated in base oil + GMO....34

Figure 5.14. a) Wear scar image and dimensions on W-DLC coated steel ball lubricated in base oil + soot b) Relevant Raman Spectra taken in specified points on the wear scar image....34

Figure 5.15 3D profile of the wear scar on W-DLC coated steel ball lubricated in base oil + soot.... 35

Figure 5.16 Schematic representation of the adsorption of mono-molecular layer in the DLC surface....35

Figure 5.17 a) Wear scar image and dimensions on W-DLC coated steel ball lubricated in base oil + soot + GMO b) Relevant Raman Spectra taken in specified points on the wear scar image....36

Figure 5.18 3D profile of the wear scar on W-DLC coated steel ball lubricated in base oil + soot + GMO....36

List of tables

Table 3 1 Content values for engine and exhaust soot..12

Table 4.1. Equipment used...17

Table 4.2. Test parameters...17

Table 4.3. Material used...17

Table 4.3. Set of 4x3 test cases..18

Table 4.4 Deposition conditions of Ag-DLC films...20

Table 4.5 – Chemical composition of Ag-DLC coatings performed by WDS.......................21

Table 4.6 – Values of LC1, LC2 and LC3 of the several scratches using load increment between 10 and 50 N...22

Table 4.7 – Chemical composition of Ag-DLC coatings performed by WDS.......................23

1. Introduction

1.1 Automotive Industries

One of the fast moving and global markets is known to be the automotive industry, in 2015 it was valued 1,653.7 billion USD. Energy efficiency, environmental impact and safety are the main fuel innovation for the automotive industry. In an increasingly competitive market, research organizations, car manufactures, and part suppliers are regularly involved in development and extensive research hoping that new innovations will be the reason for them to stand out. As an effective increase of safety and environmental concerns surrounding the automotive industry, there are demanding standards for fuel efficiency, durability and safety.

In order to decrease the fuel required to power a vehicle and increase the efficiency it is very important to minimize the energy losses from cars. Taking into consideration that a high percentage of the energy losses comes from the vehicle's engine, optimizing the performance of the engines stays as an ideal place starting to improve fuel efficiencies. One way to improve energy efficiency of a vehicle's engine is by improving its tribological performance. [1][2][3][4]

1.2 What is Tribology?

The word itself "Tribology" comes from the Greek language meaning "the study of things that rub". It is the science and engineering of interacting surfaces in relative motion and the practices thereto [5]

1.3 Introduction to Friction

When two solid materials in contact resist each other's reciprocal movement the resistance is called "friction", the resistant force that arises in that moment is called "friction force". Tribology is the main discipline in science that studies this interaction. The friction forces is separated in static and kinetic friction. The first one refers to internal movement while the second one to the resistance against motion. The grates friction is usually generated just before movement. The coefficient of friction (μ) is obtained while dividing force (F) by the vertical load (L), the intensity level of resistance is expressed with the coefficient of friction (COF). [6]

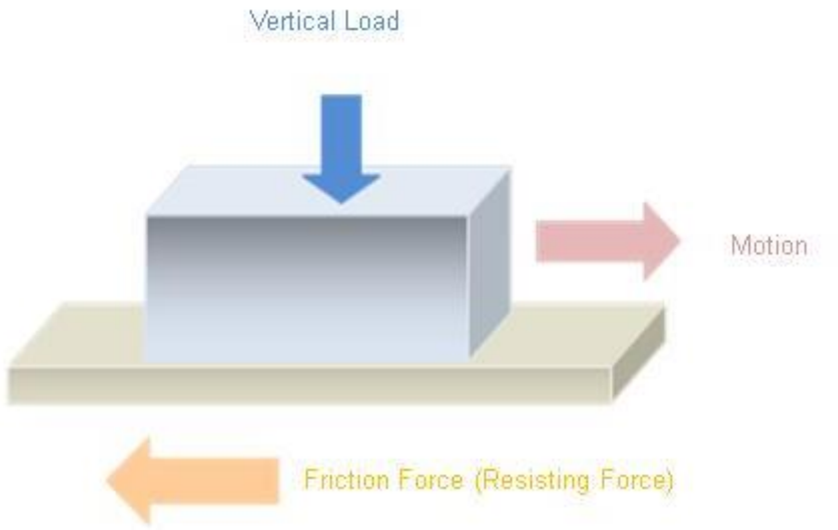

Figure 2.1 Schematic representation of friction force

1.4 Introduction to Wear

Wear is a process of material removal from a solid surface as a result of another solids mechanical actions. It occurs as a progressive loss of material when to solid surfaces are acting under load. Wear is characterized in four basic types; adhesive, corrosive, abrasive and surface fatigue. The most common type of wear is named adhesive wear, which occurs from the adhesive forces generated at the interface of the solid materials in contact. Abrasive wear happens when a hard material slides over a soft material. Abrasive wear can happen as well if a high-speed stream of liquid would hit the surface of a material. We will have corrosive wear in cases when a surface is left exposed by the sliding process and is chemically “attacked” by gas or liquid. Surface-fatigue wear happens by repetitive high stress on a rolling motion, it will cause subsurface cracks that later on will grow, removing large particles from the surface.[7]

1.5 How is the engine affected by Tribology?

An internal combustion engine’s function depends on upwards of 150-200 moving parts that operate reliably between 5000 and 50,000 hours in application ranging from a passenger car to a large commercial vehicle. If we do not understand the principles of tribology and its applications, the chances that an engine would operate smoothly are very small.

Improving the tribological properties of many tribology components in the engine including, pistons, transmissions, bearings, gears and clutches as well as additives can increase the engine power outputs, improve durability and in addition reduce fuels consumption, oil consumption and vehicle maintenance. There are several ways of improving tribological performances like: enhancing the tribological properties of the materials used for the mechanical parts; coating the surfaces; or developing lubricants that will improve the tribological behavior. [5]

1.6 Motives for tribological design and innovation

Meanwhile the first oil crisis in 1971, when oil price effectively multiplied overnight, the price of crude oil has continually risen and with it the concerns about the environmental impact as well. Today, as designers are striving to improve fuel economy, CO_2 emissions from engines has become a progressively important aspect of the engine design. For example:

- So that the drivability of the vehicle is improved, a high engine torque at low speed is demanded. This will generate very low oil film thickness in lubricated parts, particularly in turbocharged diesel engines for connecting rod bearings and crankshaft.
- Biofuels are introduced to supplement fossil fuels. Using alternative fuels, focusing finding their way into lube oil as with post-injection, plays a high role on the oil properties and henceforth component tribology.
- It must be taken into consideration the effect changes in combustion on the lubricant. A high content of soot in oil can cause significantly increased wear rates on the rings and other engine components etc.

The main effect in between all those changes is that oil films are thinner, and the components will spend a great proportion of time running at or close to a mixed - boundary lubrication regime, making the tribological environment much more challenging. Approximations from different sources for a break down in engine-friction [8] suggested that the mechanical losses in an engine are equivalent to 40% of engine output originated from the power conversion system (PCS). Thus, if reducing the friction to zero, would improve fuel economy by around 16%.

1.7 What is soot and why is it a mayor issue for the automotive industry

Currently, wear and friction represent a severe problem for the designers and manufactures. One of the main events that lead to mixed or even boundary lubrication and therefore friction and wear in the engine is the appearance of soot in the lubricant.

Soot is a carbon-based material that is formed during fuel combustion and transported through exhaust gases. The problem arises when it contaminates the engine oil at a concentration of 0.1% wt for gasoline engine oil and up to 8% wt for a diesel engine oil. Individual soot particles pose little risk to engine parts, but soot particles tend to agglomerate, eventually wear will occur. Several mechanisms by which soot causes wear are discussed below. [9]

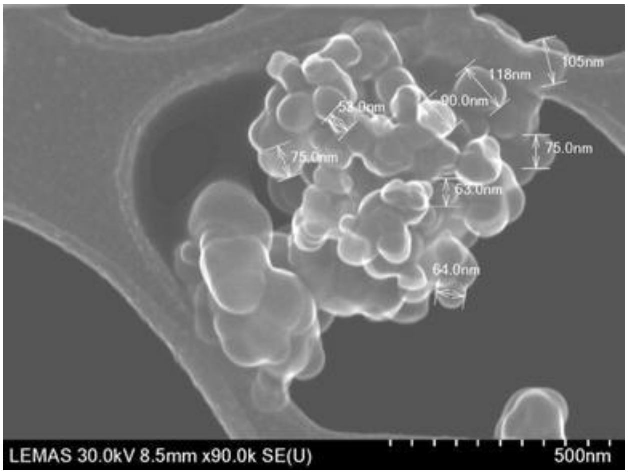

Figure 1.2 STEM micrograph of carbon black particles

i. **Competitive Adsorption**

   Here it is suggested that soot competes with antiwear additive while adsorbing into the surfaces, such an act prevents the antiwear additive to adsorb and form antiwear films. In addition, the soot particles can limit the oxygen amount that reaches the contact surface where instead of Fe_3O_4, formation of FeO oxide occurs which the last one does not have antiwear properties.

ii. **Soot Adsorbing Additive**

   While in the oil phase soot adsorbs the antiwear additives and reduces their concentration in the lubricant.

iii. **Oil Starvation**

   Accumulation of soot in the contact inlet can restrict the oil supply. Absence of the lubrication film in the contact will lead to very high wear.

iv. **Abrasion**

   Soot will enhance wear while direct abrading the metallic parts of the engine or even by removing the antiwear tribofilms formed on the surface exposing the underlying surface.

v. **Corrosive-Abrasive Wear**

   High wear (increased by 100-2000 times) is concluded to be observed when phosphorus (P-) and Sulphur (S-) based additives where added to a mineral base containing carbon black. It is concluded in the related study Olomolehin et al. [10] that wear when P- and S- based additives were added was due to corrosive abrasive mechanism.

More details about soot in engine oils will be explained later in this report. (See chapter 3.2)

2. Aim and Objective

This project aims to develop an effective response to the challenges currently faced by the automotive industry and other manufactures in decreasing the potential for more internal wear over time, due to soot-loaded engine oil.

These above aims raise the following core project objectives:

- Review literature of the effect of soot particles in internal combustion engines
- Review literature on tribological properties of W-DLC and Ag-DLC
- Analyze the coating properties of W-DLC and Ag-DLC films
- Find the suitable tribopair
- To investigate the wear occurring as a result of soot
- To experimentally evaluate the importance of W-DLC and Ag-DLC coatings against soot wear
- To investigate the effect of Glycerol Monooleate in combination with the coatings.

The long-term goal of the project is intended that the research findings will contribute in solutions for decreasing soot wear inside combustion engines in vehicles by using W-DLC or Ag-DLC thin film as a coating for the inside of the engine parts. In addition, the finding will help in the development of soot wear resistant lubricants, reduction of fuel consumption and carbon emission.

3. State of Art

3.1 Automotive engine, friction and wear reduction trends

Expending worldwide mindfulness, proven by emergency calls for control of environmental changes and greenhouse emissions, has set large new specialized commands for automotive to enhance engine efficacy. The last one being direct connected with production of carbon dioxide, and some other major greenhouse gases. Among a lot of approaches to improve engines, friction and wear reduction is one of the best and most cost-effective ways.

Recently, while science and technology in a very fast track hardware and materials are rapidly evolving. Some of the key advances that need to be mentioned are:

- Mitsubishi Introducing the first gasoline injection engine 4G9 in 1996
- In the Japanese market the Toyota Prius has been introduced in 1997
- Holset VGT^{TM} Variable Geometry (VG) turbocharger started being used in commercial vehicles in 1998.

With this speed of advancing science, the way that lubricants are being formulated and used has been changed challenging the most important factor in the automotive industry, improvement of fuel. [11][12]

In the most recent years, industries have made large steps in improving energy consumption, while lowering friction and wear in vehicles. Some of the technical solutions used in the market were the turbocharged, direct-injection spark ignition engine. But if we consider a diesel engine, utilization of the turbocharger needs to be done so it will meet strict emission regulations and improvements in the fuel economy. For the both situations engine oil technology plays a significantly role so potential problems in the market can be avoided. [13]

One of many concerns in most of the modern and well-maintained diesel engines is appearing to be soot. It oxidizes within the combustion chamber or it can be trapped and oxidize downstream in the emission system. Meeting the emission regulations by involving emission controlling technologies, visible black smoke (See Fig. 3.1) is a concern of our past. However, within the engine soot load is rising, including its presence in engine oil. [14] [15] [16]

Figure 3.1 Visible black smoke produced by old vehicles

3.2 Lubricants and Lubrication

Offering wear prevention and lowering friction are the two main functions of lubricants, making it possible to extend the lifetime of machines and thereby protecting raw materials. In certain cases, the movement of mechanical parts is just possible if a lubricant is present. Nowadays lubricants are a focus in a lot of industries because of their support on sustainability targets in economy, social and ecological areas. Their importance in reducing friction and therefore lowering the energy input plays a big role in saving emissions, in addition their wear preventive properties extends the service life and saves in terms of resources. Consisting on an average of 90% of base oils and 10% of additives, the formulation of lubricants is closely related to their applications and applications methods.

Flow properties, consistency or viscosity when referred to oils, are main parameters of creating efficiency in lubrication. Those terms appearing in almost any lubricant specifications. Friction that is created by the lubricant, surrounded by “contacting bodies” which are not in real contact shows the internal friction of the lubricant, measuring this internal friction refers us the fluids viscosity. While talking about a lubricants viscosity we might come by a term Viscosity Index (VI) which defines the lubricants viscosity-temperature behavior with the largest being at VI=100ºC and the smallest at VI=0ºC. Another common term in most international standards is the dependency of viscosity on pressure (V-p behavior). Exponential viscosity dependence on pressure means that the viscosity of the fluid will increase very rapidly with pressure. Therefore, real-world lubrication technologies consider temperature and pressure for a more accurate viscosity evaluation. [17]

3.3 Base oil

The most important component in terms of volume in the lubricant is the base oil, more than 95% of the lubricants content if formulated from it. Because of its high content, mineral lubricant base oil is considered a part of the petroleum industry. In recent years this changed due to the fact that many high-performance lubricants do not contain petroleum base oils anymore.[17] API known as the American Petroleum Institute has categorized base oils in five groups, the three first once being refined from petroleum crude oil, group IV being totally synthetic (polyalphaolefin) oils. And group V for all the oils not belonging to any of the groups from I to IV. (See Fig. 3.2) [18]

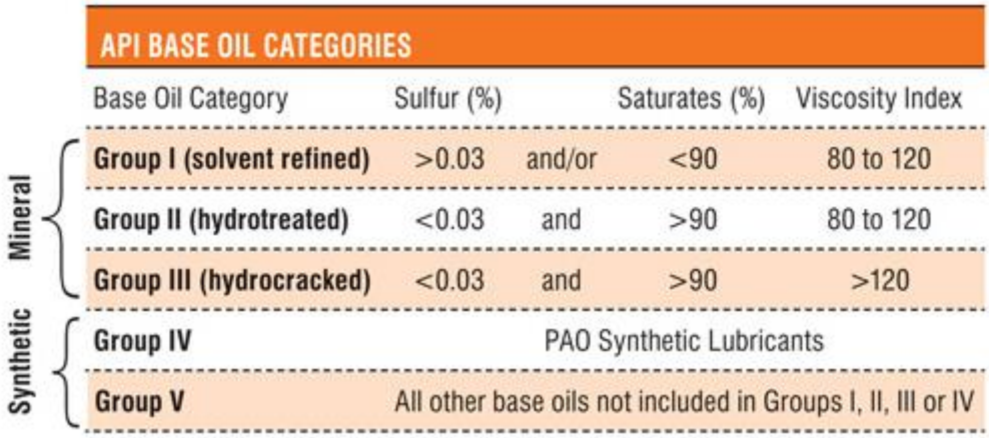

API BASE OIL CATEGORIES

	Base Oil Category	Sulfur (%)		Saturates (%)	Viscosity Index
Mineral	**Group I (solvent refined)**	>0.03	and/or	<90	80 to 120
	Group II (hydrotreated)	<0.03	and	>90	80 to 120
	Group III (hydrocracked)	<0.03	and	>90	>120
Synthetic	**Group IV**	PAO Synthetic Lubricants			
	Group V	All other base oils not included in Groups I, II, III or IV			

Figure 3.2 API base oil categories

3.3.1Ester based oil

They are base oil found in Group V that are used in different lubricant formulations. Ester based oils take more abuse when performing in high temperatures and provide superior detergency if compared to PAO synthetic base oil, increasing the hours of uses.[36] Through reaction of a carboxylic acid and an alcohol they are synthesized, and due to the chemical variety there are commercially numerous synthetic esters available. Because they differ chemically and they can be linear, saturated, breached, unsaturated, and polu-, di-, or monofunctional, they can have a wide range of characteristics. In sever conditions where lubricants with high performances are needed esters are preferred due to the properties they give. Compared to mineral oils they offer advantages of low pour points, high flesh points, higher viscosity indexes, low volatility, oxidation stability and high thermal stability, as well as an overall outstanding lubricity characteristics. A very positive point of ester-based oils are that they can be developed from plant feedstock, that makes them often a biodegradable choice and more sustainable.[19]

3.4 Additives

Engine lubricants always consist of a mixture of base oils and additive agents. Additives are various types of agents which are oil soluble. They usually are added to base liquids to strengthen positive properties, minimize unwanted properties or obtain properties that don't exists in the lubricant. [17] Different kind of additives are selected into a package to be used with a specific base oil for a specific end use application. Nowadays the largest end use is the automotive engine crankcase lubricants. Detergents, dispersants, anti-wear agents, friction modifiers, viscosity index improvers are the major functional additive types.[20]

3.4.1Glycerol Monooleate

Glycerol monooleate or for short GMO is a friction modifier. They general function is to operate under boundary lubrication conditions and lower the coefficient of friction (COF) by creating a low shear surface. Defined as surface active chemical with the ability to affect friction coefficient when a concentration of <1% is added to the base oil. They are long chain hydrocarbons with polar end groups which work by adsorbing to metal surfaces (See Fig.3.3). The coefficient of friction on those cases is affected by the operation conditions temperature, speed and load as well as the concentration of GMO.[21]

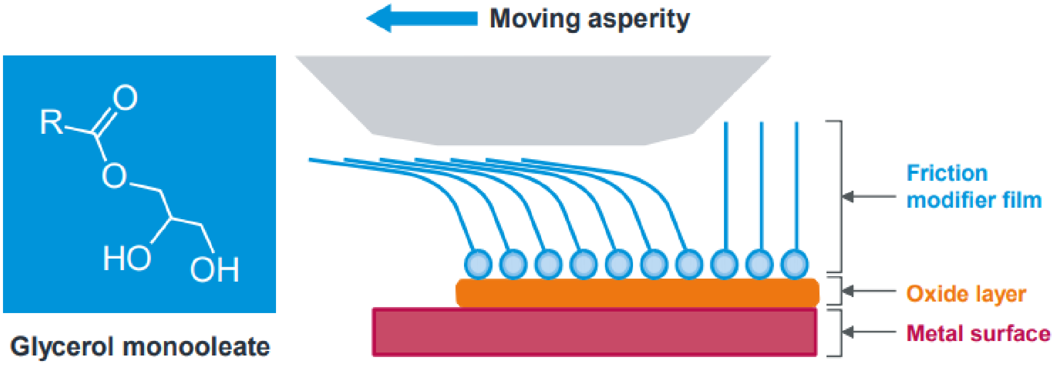

Figure 3.3 Schematic representation of working GMO

3.5 Carbon Black Soot Particles in Engine Oil

As an artefact of incomplete combustion of hydrocarbons (in this case diesel and gasoline fuel) soot is a microscopic carbonaceous particle. It is comprised of carbon, unsaturated (unburned) hydrocarbons and ash. The unsaturated hydrocarbons are essentially acetylene and polycyclic aromatic hydrocarbons (PAH). These have mainly high levels of acidity and volatility. Measurements have shown that engine soot typically contains 90% carbon, 4% oxygen, 3% hydrogen with the remainder consisting of nitrogen, sulphur and traces of meta. Measured individual or primary soot particles from diesel combustion are approximately 40nm. Since soot tends to collide the particles with a mean soot agglomerate size of 200nm can agglomerate up to a maximum, of approximately 500nm. Because of the differences in the combustion mechanisms soot particles tend to be more prevalent in diesel engines than gasoline engines. Diesel engines tend to produce greater levels of engine soot because they operate at higher air to fuel ratios. Most modem diesel engines operate using direct fuel injection and swirl within the combustion chamber to assist fuel/air mixing. Combustion starts close to the injection point and very rapidly occurs as a diffusion flame. Fuel and air will mix well in this point, since the mixture is very fuel rich it will cause very high levels of soot to be produced. After diffusion burning, through the rest of the combustion chamber by pyrolysis burning, which slowly burns most of the remaining fuel the combustion process progresses. This slow burning tends to produce more and more unburned hydrocarbons and particulates (soot) at the end of the combustion process. [22]

Soot particles are produced and destroyed throughout the combustion process; Produced by the process explained above and destroyed by oxidation. When soot or soot precursors encounter various oxidizing species oxidation will occurs. When this occurs, the particle size reduces because the hydrocarbons that are trapped inside the soot are burnt out. During the combustion process, in the initial phase of the combustion process soot particles produced contact a much higher volume of air compared to fuel, leading to a large proportion of the particles to oxidize. Further oxidation is therefore required to reduce the amount of soot finally exhausted. The combustion products when the exhaust valve opens are emitted to the exhaust system which contains more oxidizing species, that will eventually oxidize the soot. To further reduce the amount of soot emitted from the tailpipe oxidizing catalytic converters are used. Because of the oxidation of the majority of soot particles prior to exhaust, can be a possibly “why” that a large amount of soot particles are absorbed by the lubricant and relatively little is exhausted.[22]

With an increasing air to fuel ratio the concentration of the soot particles produced rises. The rate of soot production increases dramatically when the air to fuel ratio nears stoichiometric (14.5 for diesel fuel). This happens because near stoichiometric there won't be enough time and oxygen in the cycle to completely bum all the diesel fuel, as well to oxidize the soot there will be only a low proportion of oxidizing species. Generally, excessive amounts of soot are produced from the combustion process at values of 20% fuel lean of stoichiometric and higher, which are now being used. Excess air is required to reduce hydrocarbon emissions and increase diesel cycle efficiency. [22]

As investigations have shown soot emitted from the tailpipe and soot contained in the engine lubricant are quite different. The oxidation processes that the combustion products go through can be a possible reason. As mentioned, soot particles in lubricants has a low oxygen content and very high content of carbon. In table 3.1 comparison of approximate content values for engine and exhaust soot can be seen. [22]

Table 3 2 Content values for engine and exhaust soot

Soot Constituent	Engine Soot Content	Exhaust Soot Content
Carbon	90%	>50%
Oxygen	4%	<20%
Volatile content	6%	20%

3.6 Theories about soot wear

From a purely chemistry point of view, initial investigations (circa 1970's) were carried out, showing that soot was one of the contributing factors to long term oil degradation. Showing that with oil degradation the amount of wear increased in the engine components. Since at that time there was not a lot of information regarding soot, lubricant scientists assumed that it must be the reason for the degradation of the lubricant's anti-wear additives. Later, with further investigations it was found that, the elements required to produce the anti-wear function of the lubricant remained even after the soot had degraded various elements of the anti-wear additives. Prevent against various forms of engine component wear e. g. corrosion etc. is the main function of anti-wear additives, therefore wear found in combustion engines with soot contaminated lubricants should occur due to more fundamental mechanisms, such as abrasion. [22]

As research has developed in more recent years, various studies have individually highlighted polishing on a macroscopic level, due to the soot contained within the lubricating oil lubricant contact starvation and microscopic abrasion was observed. Many studies are obtaining similar findings in the recent years (2000 onwards), leading to acceptance of the theories by lubricant and engine manufacturers and considerable agreement between researchers. [22]

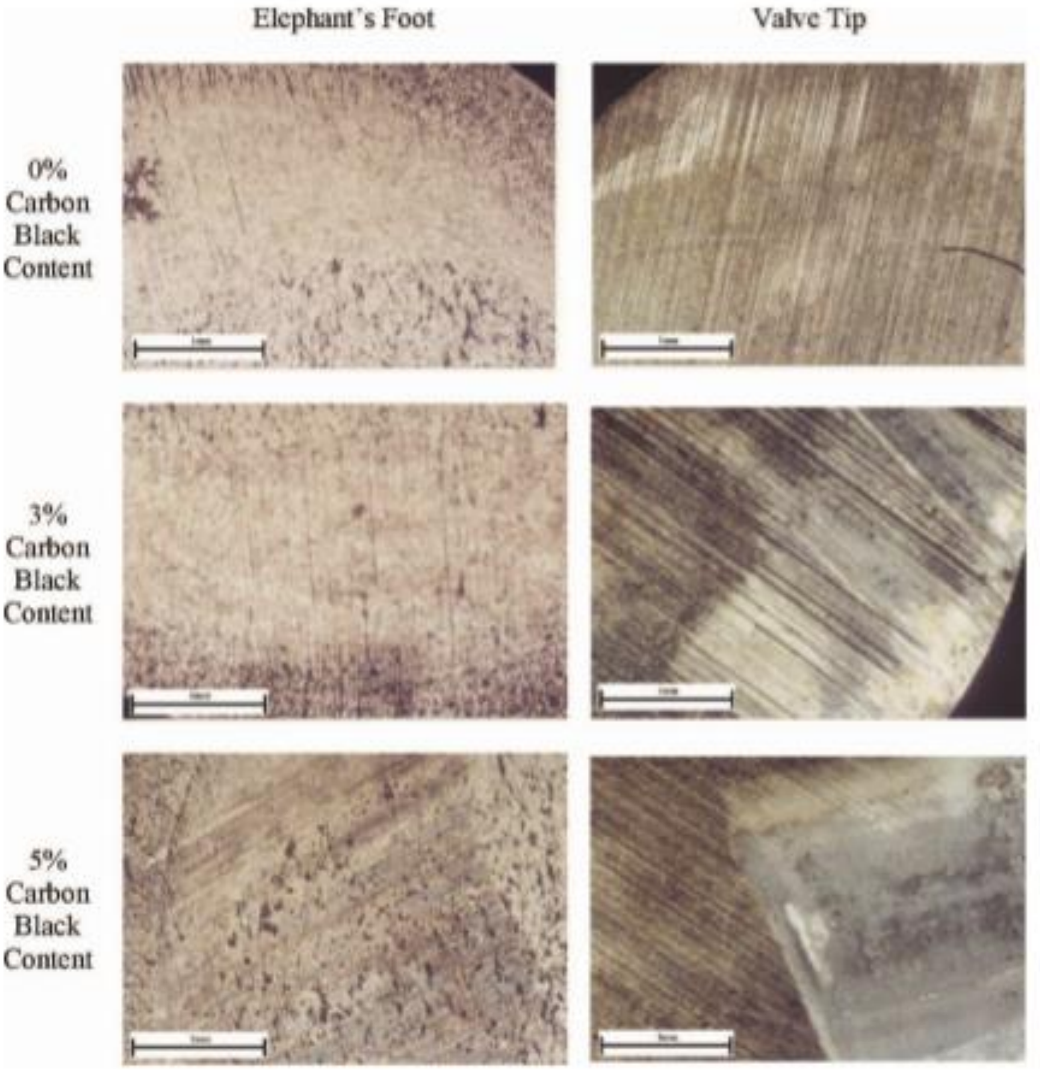

Figure 3. 4 Images of component reciprocating tests performed at 100°C [22].

3.7 Materials

3.7.1 DLC

DLC also known as Diamond like carbon is a metastable form of amorphous carbon that contains a significant fraction of sp^3 bonds. It can have high values of mechanical hardness, optical transparency and chemical inertness. They are commonly used as protective coatings in different kind of areas like car parts, biomedical coatings, micro-electromechanical devices (MEMs) etc. [23]

As we can imply by the name, DLC has the ability to provide us with the properties of diamond to the surfaces of a large selection of materials. The most and best properties that it can have is hardness, slickness and wear resistance. (Friction coefficient of DLC film against polished steel will range from 0.05 to 0.20) [24]. DLC properties depend a lot on the coating thickness, interlayer thickness, plasma treatment etc. [25]

A problem that usually occurs while depositing DLC coatings is that the internal stresses which DLC benefits the hardness from, make it very difficult to bond the DLC to the substrate which needs to be protected. Those internal stresses tend to “pop” up the coating off from the underlying surface. A possible solution to this is usually an interlayer that will increase the adhesive abilities of the coating. Another solution is the incorporation of metal atoms like titanium (Ti), chromium (Cr) or silver (Ag) to the carbon film that might reduce the residual stresses, and thus adhesion failure. [26]

Due to their very good anti wear properties DLC coatings are very popular in the field of tribology. It is very resistant when it comes to adhesive and abrasive wear making it appropriate to be used in conditions like extreme contact pressure. According to some last studies still unpublished, done by Ducom Instruments – The Tribology Company, DLC might be a possible solution to soot wear. The increase of lifespan of many products because of its tribological properties make it very beneficial for a sustainable economy.

3.7.2 W-DLC

DLC doped with tungsten (W) in recent years has shown enhanced tribological properties, resulting in a low coefficient of friction and low wear due to the inherent lubricity of the coating. Moreover, when additives were used, significant improvements in the wear resistance of the W-DLC have been reported. [27] Until now W-DLC is mainly used in bearings to improve the wear resistance and decrease heat. They exhibit high hardness and a low COF through a wide range of temperatures. In addition, the coating has excellent adhesion to the steel substrate making them very resistive against flaking or chipping.[28] Those properties classify W-DLC coating as a possible solution to soot wear.

3.7.3 Ag-DLC

Alloying DLC, with Ag (noble material) will result in the formation of a ductile and soft phases that makes it possible to improve adhesion and toughness of the coating. According to several studies Ag-DLC show an enhanced coating adhesion in steel substrates as well as reduction of the internal stresses. Ag as a soft component with preferential wear can result in creation of a tribofilm that will adhere in the worn surface and act as a solid lubricant, in the same time it could prevent soot adhesion due to its low chemical reaction properties.

X.Yu et al [29], found that if we incorporate 4.3-10.6 at.% Ag in the DLC, the coating resulted in both reduction of wear and friction coefficient, this attributed to the presence of Ag nanograins that were found in the top layer of Ag-DLC coating. [26] So, incorporating Ag in DLC films shows a promising combination to form protective layers. Those excellent tribological properties of Ag in DLC films are a result of the following factors: Since the cubic structure is face centered, Ag has much smaller elastic modulus than DLC, adsorbing compressive stresses from the DLC matrix. In addition, composite films toughness can be increased. Another reason is silver as a soft metal with low shear strength film onto a hard metal surface can decrease friction coefficient by modifying the contact interfaces to plastic flow in the process of relative slip. [30] Silver doped DLC has never been testes before as a solution to soot wear opening a new research gap that needs to be investigated.

4. Experimental details and characterizations

4.1 Tribological Testing

4.1.1 Equipment set-up and test parameters

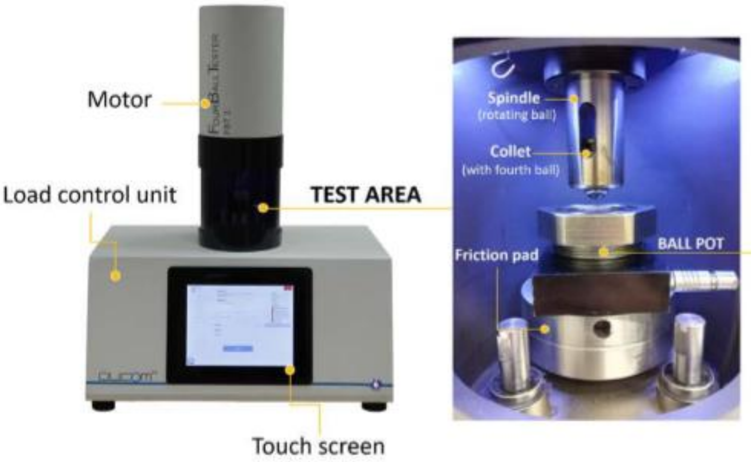

Figure 4.1 4 ball tester working environment

The Automated DUCOM four ball tribometer shown in Fig 4.1 was used to measure the wear preventive (WP) properties of both the lubricant and coatings as well as measure the coefficient of friction (COF). The tribometer consists of a collet in the top which is used to hold and rotate the top ball at a desired speed. In the vertical direction the top ball is stationary. In the bottom, a ball pot where three balls are placed, and the desired lubricant is poured, is screwed to resist any motion. [31] A thermocouple and heater found in the ball pot are used to heat the oil, then measure and maintain the desired temperature. The ball pot containing the fixed balls and lubricant is than pressed against the upper ball with a defined load that is controlled by a load control unit, compromised of pistons, pneumatic chambers, and normal load sensors [31]. A schematic representation of the test area is shown in Fig.4.2

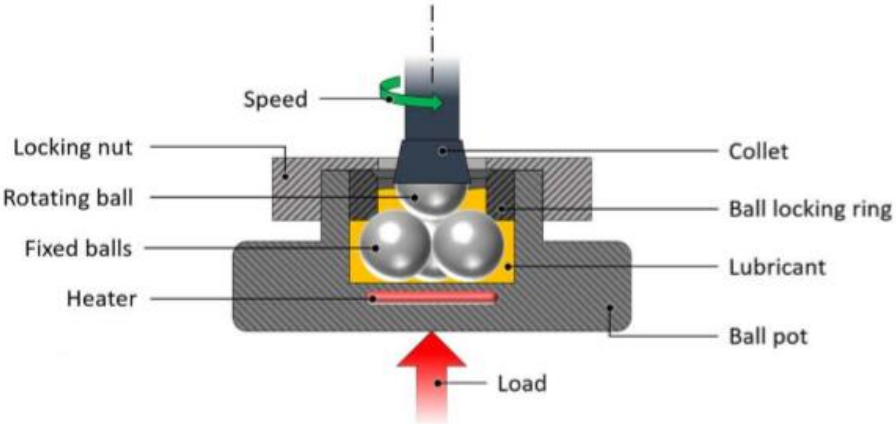

Figure 4.2 Schematic representation of the 4 ball collet set up

The tests were performed according to the Standard Test Method for Wear Preventive Characteristics, Designation D 4172-94. The four ball tribometer model can be found in Table 4.1 while the Test parameters are listed in Table 4.2. All the data are being displayed in real time and recorded using a LabView based WinDucom software.

Table 4.1. Equipment used.

Name and model of tribometer	Manufacturer	City and country
Four Ball Tester (FBT-3)	**Ducom Instruments**	**Bangalore, India**

Table 4.2. Test parameters

Test parameters		
Normal Load	**N**	**392 ± 1**
Temperature	**^{0}C**	**75 ± 1**
Speed	**rpm**	**1200**
Test Duration	**s**	**3600**

4.1.2 Materials and preparatory procedures applied

12.7 mm diameter steel balls made of chrome alloy steel following AISI E−52100 standard and, hardened to 64–66 HRc (Rockwell C Hardness) where used. For the coated balls, to not affect the coating Ultrasonic Cleaning was avoided, although before each test the coated balls were immersed in isopropanol and cleaned with industrial wipes three times to make sure no debris are left, air drying followed. The uncoated balls were ultrasonically cleaned in a sonic bath containing acetone for 10 minutes, after they were immersed in isopropanol and air dried, the same procedure was done before each test for the ball pot and the collet as well. The materials used are listed in Table 4.3.

Table 4.3. Material used.

Test Balls	Diameter	Standard	Coating
Steel Balls	**12.7**	**AISI E-52100**	**Uncoated**
Steel Balls	**12.7**	**AISI E-52100**	**W-DLC**
Steel Balls	**12.7**	**AISI E-52100**	**Ag-DLC**

The base oil used during the tests was ester base oil (Radialube 7250) with the properties listed in Annex A. Afterword, additive (See Annex A) was added, the base oil was mixed with 1% of Glycerol Monooleate (GMO) using a magnetic stirrer for 30 min at 70ºC. To observe the effect of soot, carbon black was introduced to the both lubricants, base oil and base oil and Additive Mixture. Carbon black or CB type Vulcan XC72R (Cabot Norit Netherlands B.V., the Netherlands) because of its similarity in carbon content, particle size (30nm to 50nm) and morphology was used as a surrogate to engine soot. However, we need to mention that, compared with the real engine soot (Otto or diesel) the surface chemistry of CB cannot be compared since engine soot has higher concentration of functional groups. We have selected CB in our experiments for the main purpose of repeatability. From now on, any time we use the term “soot” we are referring to carbon black. By stirring the soot particles in engine oil at 70ºC for 30 min, engine oils with 1 wt % of CB was prepared.[33] A set of 4x3 test cases was created which is listed in Table 4.3.

Table 4.3. Set of 4x3 test cases.

Oil	Upper and Bottom Balls setup 1 on 3		
Radialube 7250	**STEEL on STEEL**	**Steel on W-DLC**	**Steel on Ag-DLC**
Radialube 7250 +1% GMO	**STEEL on STEEL**	**Steel on W-DLC**	**Steel on Ag-DLC**
Radialube 7250 + 1% Carbon Black	**STEEL on STEEL**	**Steel on W-DLC**	**Steel on Ag-DLC**
Radialube 7250 + 1% GMO +1%	**STEEL on STEEL**	**Steel on W-DLC**	**Steel on Ag-DLC**

4.2 Coatings

4.2.1 DC Magnetron Sputtering

For the deposition of DLC the most common industrial process is sputtering. DC (direct current) is the most common form of sputtering of a graphite electrode by an argon (Ar) plasma. Since graphite has a low sputtering yield, magnetron sputtering will be used so the deposition rate can be increased. [23]

Magneton Sputtering is a Plasma Vapor Deposition (PVD) process where a plasma is created, an electrical field superimposed on the negative charged electrode or “target” will accelerate the positively charged ions. The ions are accelerated by potentials that range from a few hundred to a few thousand electron volt (eV) and will strike the electrons with enough force to bombard and eject atoms from the target. From the face of the target the atoms are ejected in a typical line-of-sight cosine distribution which after they will condense on the surface which is placed in proximity to the magnetron sputtering cathode. Depending on materials that one subsequently wants to deposit on the surface, appropriate targets are created. Because of its versatility, its widespread use to sputter a large selection of materials, and its ease of scale up, sputtering is preferred for industrial application. [33] The equipment is composed by a cylindrical deposition chamber with a diameter of 40cm and high of 44cm, gas flow control, vacuum pumps and electrical systems. Inside the chamber the target was supported by two parallel cathodes. A schematic representation of the DC Magnetron Sputtering Machine can be seen in Fig. 4.3.

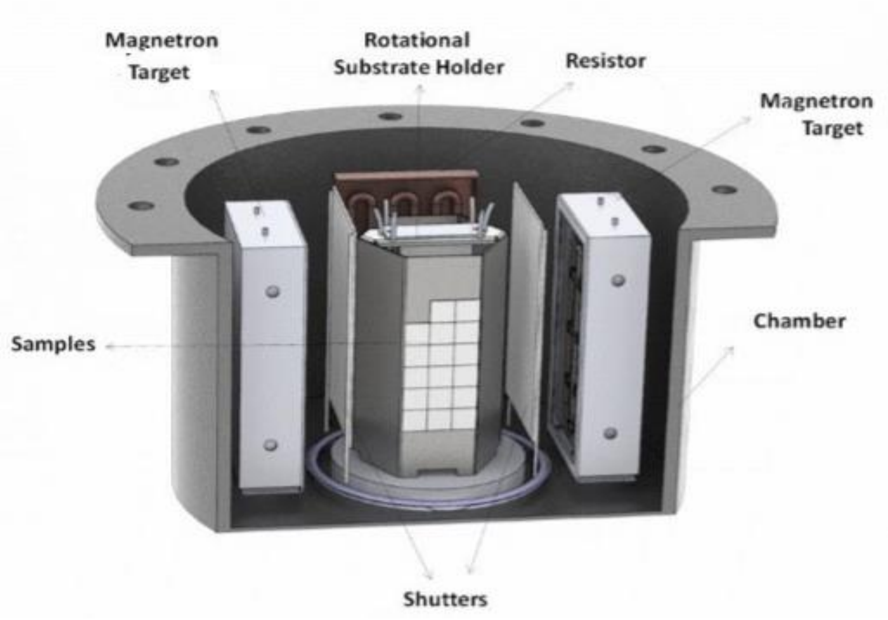

Figure 4. 3 Schematic representation of DC Magnetron Sputtering

4.2.2 Ag-DLC Coating Deposition

The Ag-DLC coatings using DC Magnetron Sputtering were deposited using 22 high purity silver pallets (99.99% of purity) each one approximately 25mm^2 of area and 3 mm of thickness, which were incorporated in the erosion zone of the pure graphite (99.99% of purity) pallet with dimensions of 200 x100 mm^2. The second target was chromium pallet (99.99% of purity) which will be used to produce an interlayer to increase adhesion between the coating and the substrate. Before the deposition, all the substrates were cleaned in an ultrasonic bath, in acetone and ethanol for 10 min. The balls that were about to be coated were normally place on a plate with cavities and glued with silver glue. The substrates including the samples were placed in the center of the cylinder at about 15 cm of the target. Two vacuum pumps made it possible to achieve pressure around 2.7x10^{-3} Pa before the deposition. The substrate holder during the deposition was electrically biased (-50V). During the coating process the working gas (Argon-Ar) was introduced causing a work pressure of 3.8x10-1Pa, while the substrate was rotating in a constant speed of 10rpm. The conditions are described in Table 4.4.

Table 4.4 Deposition conditions of Ag-DLC films.

Steps	t (s)	Ar_{main} chamber (%)	P_{MAG1} (W/cm^2)	P_{MAG2} (W/cm^2)	V_{Subs} (V)	t (pulse) (μs)	f (KHz)	P (Pa)
Etching Target MAG1 + Subs	600	15	1.75	0.25	500	1.6	250	4.96E-01
Etching Target MAG2 + Subs	600	15	0.25	3.38	500	1.6	250	5.00E-01
Interlayer deposition	450	12	0.25	3.38	50	0.5	250	3.87E-01
Transition Interlayer	600	12	6.00	0.25	50	0.5	250	3.90E-01
Deposition	5400	12	6.00	0.25	50	0.5	250	3.80E-01

4.2.3 W-DLC Coating Deposition

W-DLC coatings have been prepared in Instituto Pedro Nunes in Coimbra, Portugal. They have been prepared without my presence and been available for testing further on. The characterizations of the coating can be found later on this report.

4.2.4 Ag-DLC coating characterization

Using Scanning Electron Microscope (SEM) JEOL model JSM-5310 the thickness and cross section morphology were inspected. As seen in FIG X the coating is about 1.35 um thick. As observed, it more a compact structure which is not usual for DLC coatings.

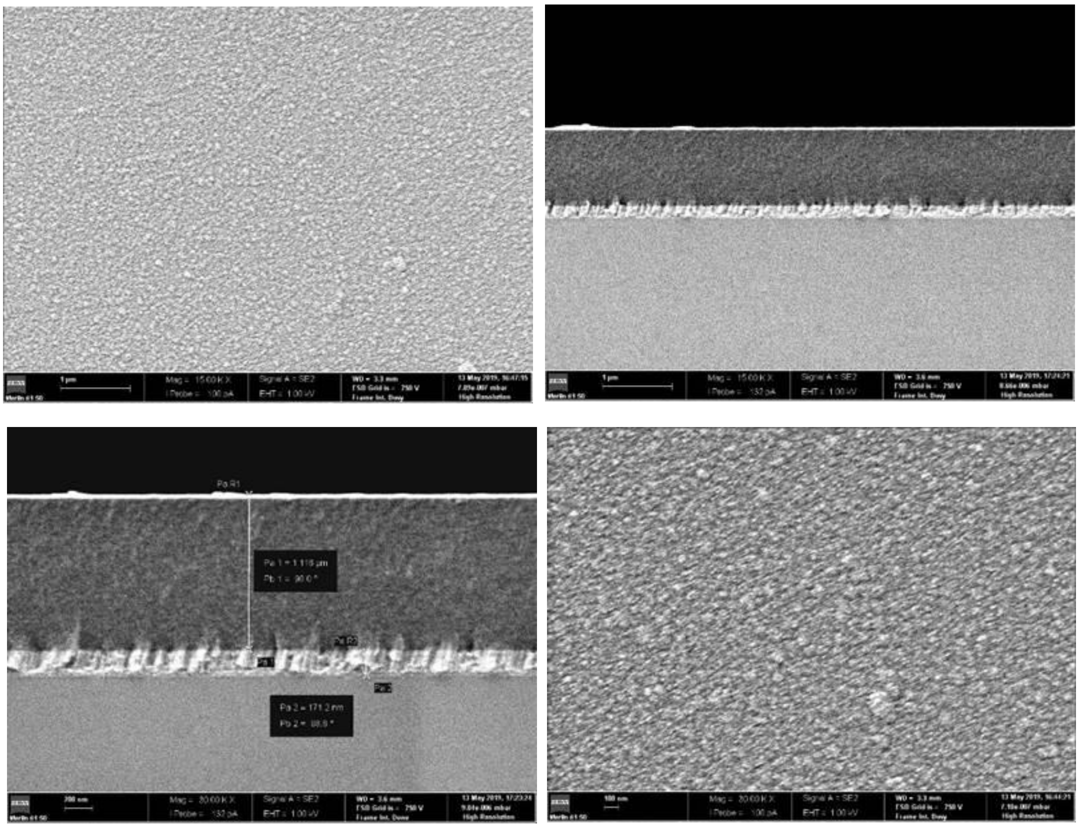

Figure 4.4 Scanning Electron Microscope (SEM) images of the thickness and cross section morphology of Ag - DLC

By using Wavelength Dispersive Xray Spectrometer (WDS) which is coupled to SEM the chemical composition was analyzed. At a magnification of 1000x (area of approx. 112x85 um2), current beam of 65nA, an acceleration voltage of 10kV and a work distance of 8mm, three measurements were done on the samples surface. The results (Table X) showed about 5-7% of at. % Ag considering that WDS does not identify the chemical element Ar.

Table 4.5 – Chemical composition of Ag-DLC coatings performed by WDS

	% at. Ag-DLC
Ag	7.77
Si	0.073
O	1.355
C	91.404
Cr	0.076
Ar	

Hardness

Using nanoindentation test were a controlled load is pressed by a hard tip into the Ag-DLC coting, hardness was measured. MicroMaterialsNano test aparatures operating with a Berkovich indentor was used for two different loads tested, 5 and 10 mN. The hardness of the coating resulted to be respectively 11.24 (±0.46) GPa and 12.01 (±0.55) GPa

Adhesion

To evaluate the adhesion of the coating a conventional scratch test with a diamond, radius of 200 um (CSEM Revetest) was performed. While observing the scratch with an optical microscope the critical load was determined. AISI-M2 steel substrate was used for comparing reasons with other systems. The coating delaminated at 54.7 (±4.8) N, see Figure 4.5 and Table 4.6.

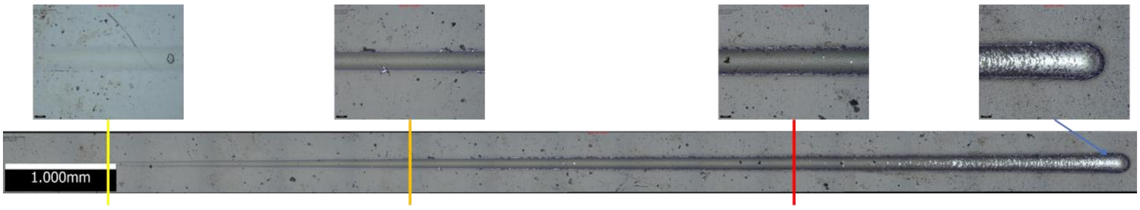

Figure 4.5 Scratch test of Ag-DLC with the identification of the zones of cohesive failures (yellow) and adhesive failures (orange and red) being the red one indicative of the delamination zone of the coating from the substrate.

Table 4.6 – Values of LC1, LC2 and LC3 of the several scratches using load increment between 10 and 50N.

	LC1 **(N)**	**LC2 (N)**	**LC3 (N)**
Scratch 1	7.7	32.9	61.9
Scratch 2	9.2	36.2	51.8
Scratch 3	8.3	28.1	62.8
Scratch 4	8.1	32.6	54.3
Average scratch	**8.3 (±0.6)**	**32.5 (±2.9)**	**57.7 (±4.8)**

4.2.5 W-DLC coating characterization

To observe com surface and cross section morphologies and to evaluate the chemical composition a scanning electron microscope (SEM) (ZEISS Merlin – Field Emission Gun) equipped with energy dispersive spectroscopy (EDS) was used. Results are shown in Fig. 4.6 and Table 4.7

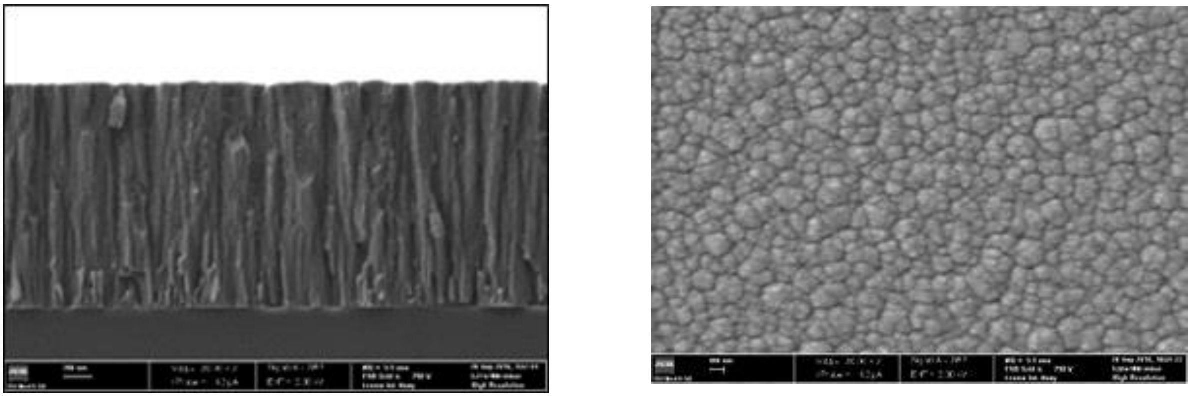

Figure 4.6 SEM images of the thickness and cross section morphology of W - DLC

Table 4.7 – Chemical composition of Ag-DLC coatings performed by WDS

Sample	C (at. %)	W (at. %)	Ar (at. %)	O (at. %)	Thickness (nm)
DCMS	82.2	14.6	2.6	0.6	1730

By scratch (See Fig.4.7) test with a Rockwell indenter with diamond tip of 200 µm radius with standard conditions from 0 to 50 N the coatings adhesion was evaluated. The scratch was analyzed by optical microscopy. Mechanical properties, reduced Young modulus and hardness were measured by depth-sensing indentation (MicroMaterials NanoTest platform). 10 mN of maximum load was selected in order to avoid the influence of the substrate with the maximum indentation depth, it never reaches values higher than 1/10 of the coating thickness. The hardness results showed 14.3 (+/-0.9) GPa and the reduced young modulus obtained was 168 (+/-5.65) GPa

Figure 4.7 Scratch test on W-DLC with the identification of the zones of cohesive failures (yellow) and adhesive failures (orange and red) being the red one indicative of the delamination zone of the coating from the substrate.

4.3 Post test analyses

4.3.1 Optical Microscopy

Often referred as “light optical microscope” the optical microscope is a type of microscope that uses a system of lenses and visible light to magnify images of small samples. The wear scar images for our samples have been taken using an optical microscope from AmScope, measurements of the wear scar have been done using its AmScope software. [34]

4.3.2 3D Profilometry

Profilometry is used to extract 3D topographical data from the surface, on request it can be a line or a single spot scan as well. Its purpose it to get the morphology, surface roughness and step heights. The optical profilometer used to scan the wear scar after the 4 ball tester was from Filmetrics. It uses light to create a 3D scan of the surface. Examples are optical interference, using a focus and detection, confocal aperture, and projecting a pattern in an optical image, A schematic interpretation can be seen in Fig. 4.8 The images after, have been analyzed using Profilm Online.[35]

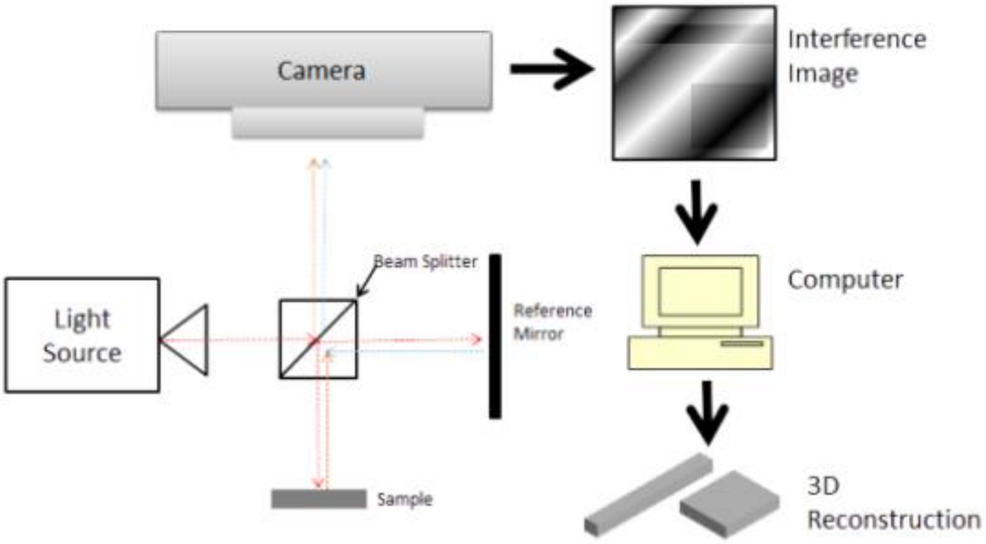

Figure 4.8 Schematic of an Interferometric profilometer [35]

4.3.3 Raman Spectroscopy

Based on inelastic scattering of monochromatic light usually from a laser, Raman spectroscopy is a spectroscopic technique. Inelastic means that upon interaction with a sample the frequency of photons in monochromatic light will change. In comparison with the original monochromatic frequency, the frequency of the reemitted photons is shifted down or up, this is called the Raman effect. The shift will provide information about rotational, vibrational and other low frequency transitions in molecules. It can be used to study gaseous, liquid and solid samples. The sample is illuminated with a laser beam in the near (NIR), visible (Vis), or ultraviolet range (UV). The light that is scattered will be collected with a lens and passes through interference filter or a spectrometer so Raman spectrum can be obtained.[36] Raman spectroscopy provides key information about material structure and chemical composition.

The equipment used to obtain our Raman Spectra is a Jobin Yvon (Horiba group) HR800. The spectra were collected with the following parameters: laser line of 441.6 nm, 600 grooves/mm grating, iris aperture of 0.25 mm, objective lens of x100 magnification and NA=0.9, integration time of 2x10 (2 accumulations). Before Raman the tested balls have been cleaned properly with isopropanol. The spectra after, have been analyzed using OriginPro 8.5 software and literature-based data. A schematic representation of Raman Spectroscopy work flow is shown in Fig. 4.9

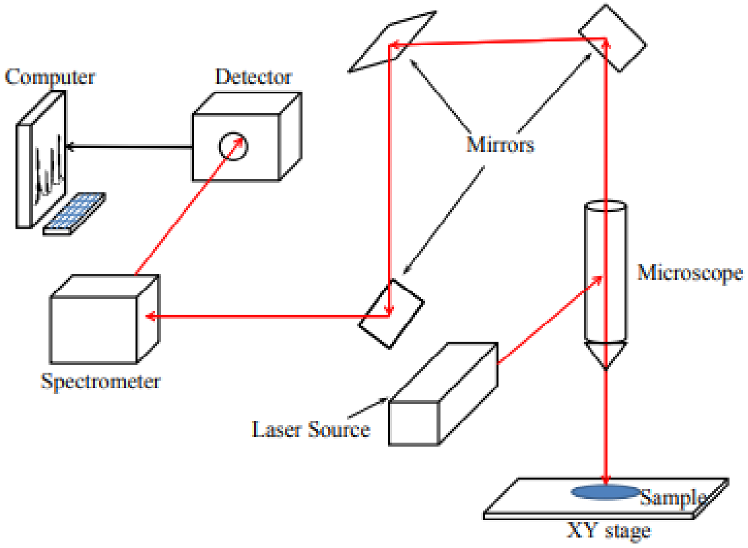

Figure 4.9 Schematic representation of Raman Spectroscopy work flow

5. Results

5.1 Tribo-pair set up

Before testing the coating properties we did a reasearch on the set up that will be used. As the 4 Ball tester uses 4 balls (1 moving, 3 fixed), 3 set ups have been availabel: 1 steel ball against 3 DLC, 1 DLC against 3 other DLCs and 1 DLC against 3 steel balls. The same test conditions have been used as chosen for the wear preventive test done afterwards to test the coating properties (See Table 4.2) as well as the same base oil. The friction coefficeient for all the set ups is shown in Fig 5.1, as we can observed the lowest COF was obtained from the upper moving ball steel and 3 fixed DLC balls contact. In addition we can see that using a uncoated counterbody led in both cases to lower friction then using a DLC on DLC contact, benefiting the economy as well.

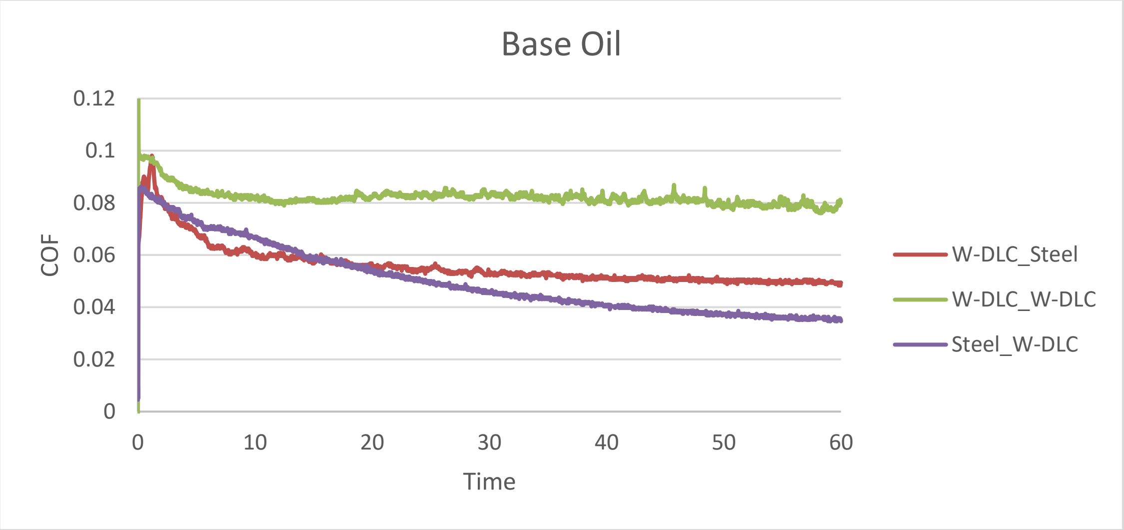

Figure 5.1 Coefficient of friction from 3 different tribo-pair set ups lubricated in base oil.

Since the W-DLC on Steel and Steel on W-DLC almost achived the same coefficient of friction wear analyses have been done aswell (See Fig. 5.2). The last one showed better result in the case of wear preventive properties. To make sure that the counter body did not experience in this case a lot of demage, we used an optical microcsope (Fig. 5.3) and a 3D Profilometer (Fig. 5.4) to observe the wear scar in the upper steel ball. As the results where quite satisfying and no serious wear was detected we decided to continue with the uper steel ball on 3 bottom DLC balls set up to testing the coatings.

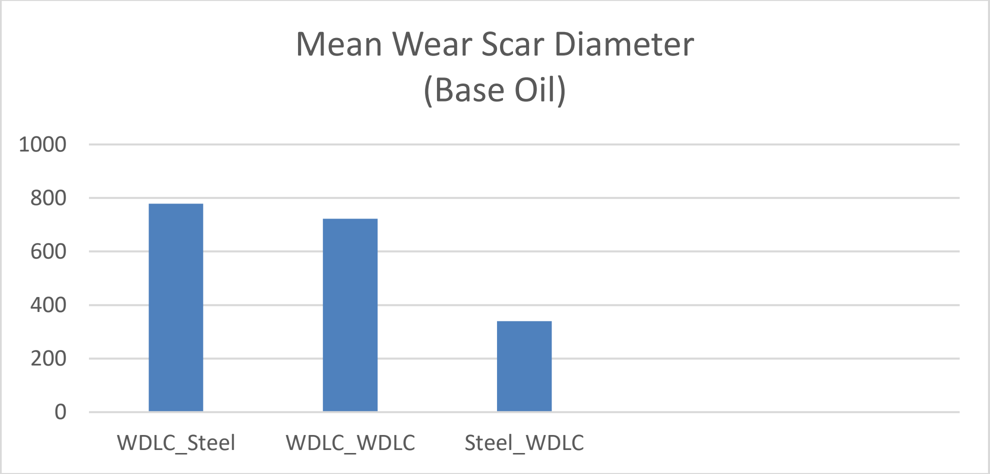

Figure 3.2 Mean Wear Scar Diameter from 3 different tribo-pair set ups.

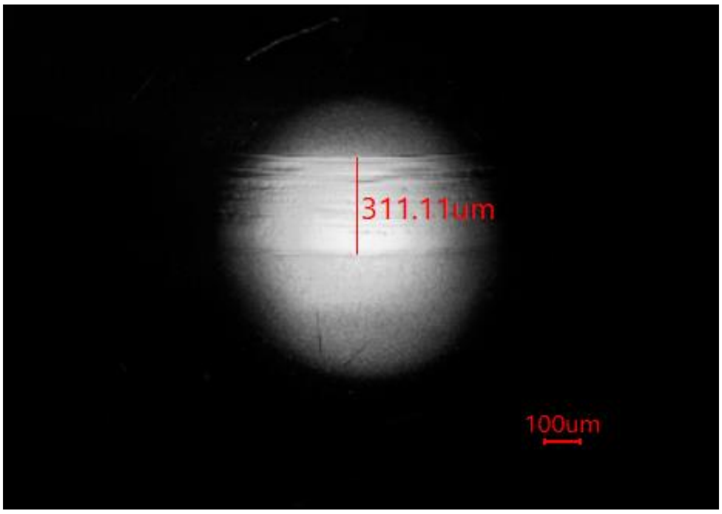

Figure 5.3 Optical image of the wear scar from the upper steel ball in the steel-WDLC set up lubricated in base oil.

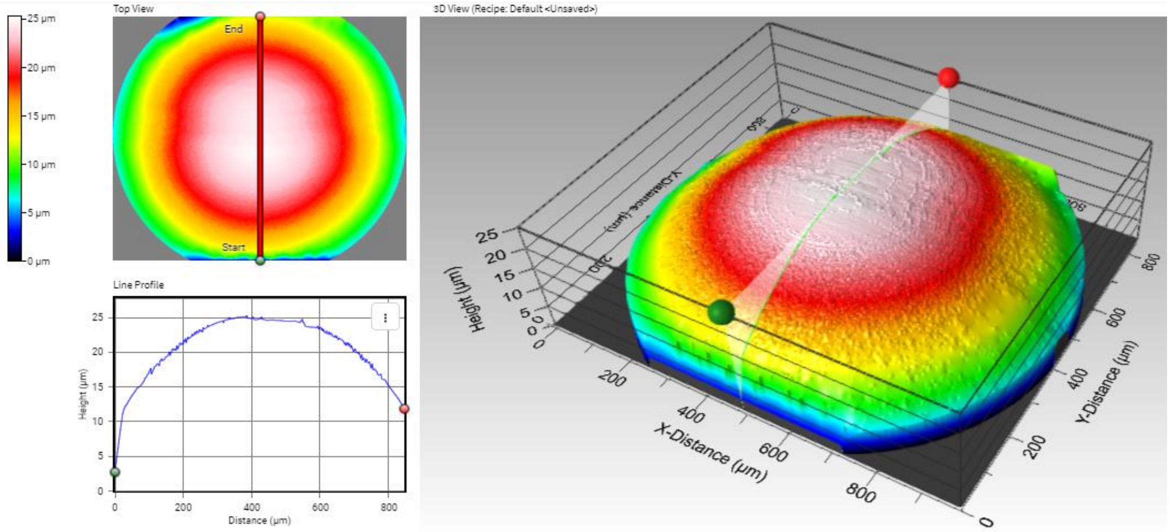

Figure 5.4 3D profile of the wear scar from the upper steel ball in the steel-WDLC set up lubricated in base oil

5.2 W-DLC

5.2.1 Friction evaluation

Lubricated in the formulated oils listed in Tab. 4.3 , friction results for W-DLC have been shown in Fig. 5.5 For all the formulated oils the coefficient of friction (COF) remained stable throughout the experiments, friction respond did not show any discontinuety or sudden changes. We could observe that GMO did not have any significant effect in the reduction of the coefficitent of friction if we compare it to the results obtained for steel/W-DLC contact when lubricated in only base oil. While for the base oil lubricated test the coefficient of friction reached 0.05, adding GMO resulted the same COF of 0.05. This might be a result of the small amount of the friction modifier. Similar results where obtained in earlier studies from L.Yang.[37] We noticed that the base oil containing only 1% of Soot showed the lowest friction coefficient (0.042), this reduction of friction can be attrebuted to higher stresses induced from the soot particles helping sp2 hybridization in the coating explained later in this report. When we added both of the factors (1%Soot+1%GMO), COF rised slightly to 0.047.

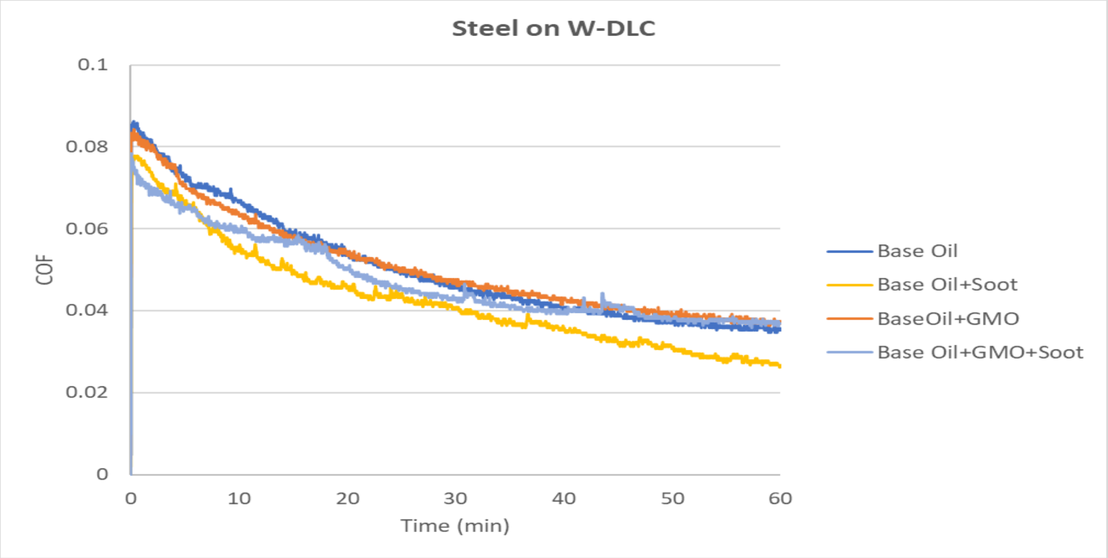

Figure 5.5 Coefficient of friction obtained from the 4 ball tester for steel and W-DLC tribopair lubricated in base oil, base oil containing 1% GMO, base oil containing 1% of soot and base oIl containing 1% GMO and 1% soot.

However, if we compare the COF of steel/steel contact to the tests with steel/W-DLC contact, we notice a big difference. Test performed in base oil for steel/steel contact reached a friction value of 0.9, while steel/DLC a COF of 0.05, showing the benefits of the coating in the system since no additive was present. Steel/WDLC showed better results compared to stee/steel for all other formulated lubricants as well.The COF for steel/steel contact compared to steel/W-DLC, for the base oil are shown in Fig 5.6 while for all other formulated lubricants they can be found in ANEX B

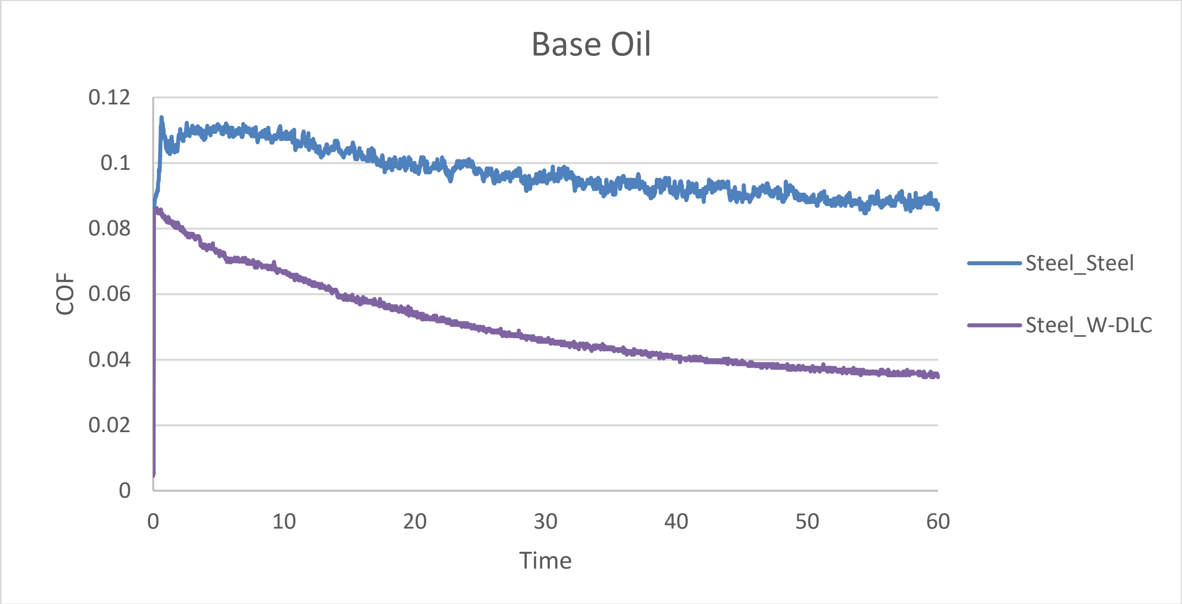

Figure 5.6 Coefficient of friction obtained from the 4 ball tester for steel on steel and steel on W-DLC tribopair lubricated in base oil.

5.2.2 Wear results

Mean wear scar results are presented in Fig5.7 .The mean wear scar diameter was measured for all the three bottom balls of the 4 Ball tester. Results show an increase of the wear scare from 339 to 390 µm when soot was added.The wear on the surface related to soot was visible in the 3D profile of the ball where in some parts the depth of the wear scar exceeded the coating thickness (See Fig.9). [37] Compared to steel on steel tribo-pair the mean wear scare was reduced from an average of 678 to 353µm.

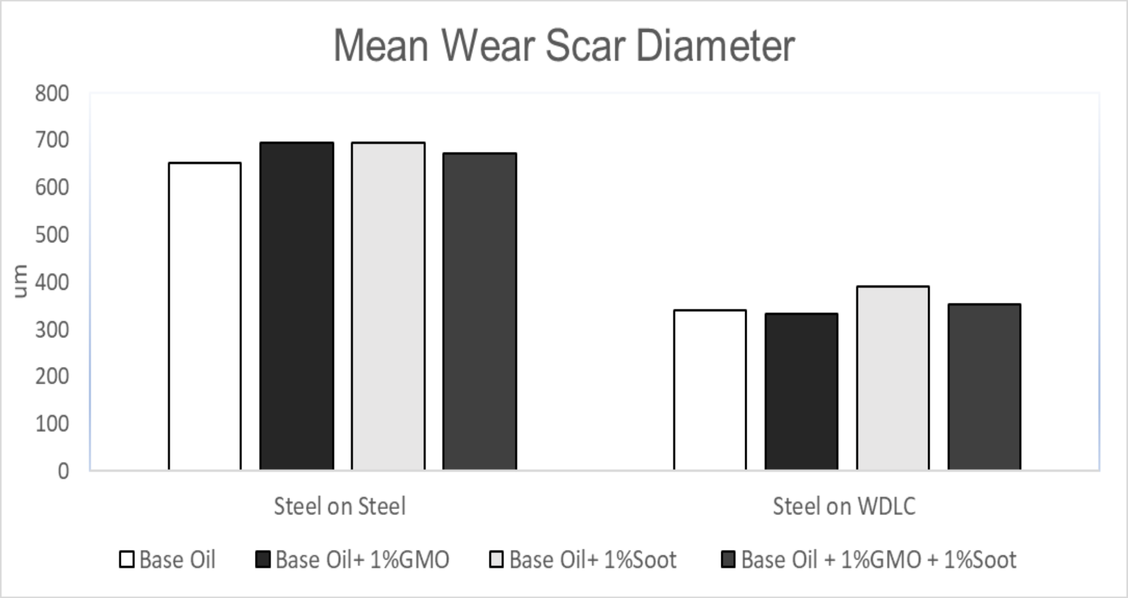

Figure 5.7 Mean wear scar diameter obtained with an optical microscope and measured with AMScope software for steel on steel and steel on WDLC tribopair lubricated in all formulated oils.

5.2.3 Raman Results

In University of Aveiro, Raman analyzes have been performed within the wear scar on the uncoated steel balls to see potential peaks from the substrate as well as for coated steel balls to see if any change in their coating structure have occurred.

At Fig. 5.8 we have the Raman results from the wear scar on the uncoated steel balls from the steel/steel contact, as we can see iron oxide peaks rising at 668 cm^{-1} belong to Fe_3O_4 while the once at 299, 613 cm^{-1} to Fe_2O_3 formed in the surface.[38] Those oxides are well known to reduce friction but because of their hardness they enhance wear.[39]. Since the balls were cleaned properly before the test, we cannot see any rise of the G peak in the case where soot is involved. In addition, the image of the wear scar obtained with an optical microscope shows visible wear on the surface (See Fig.5.9)

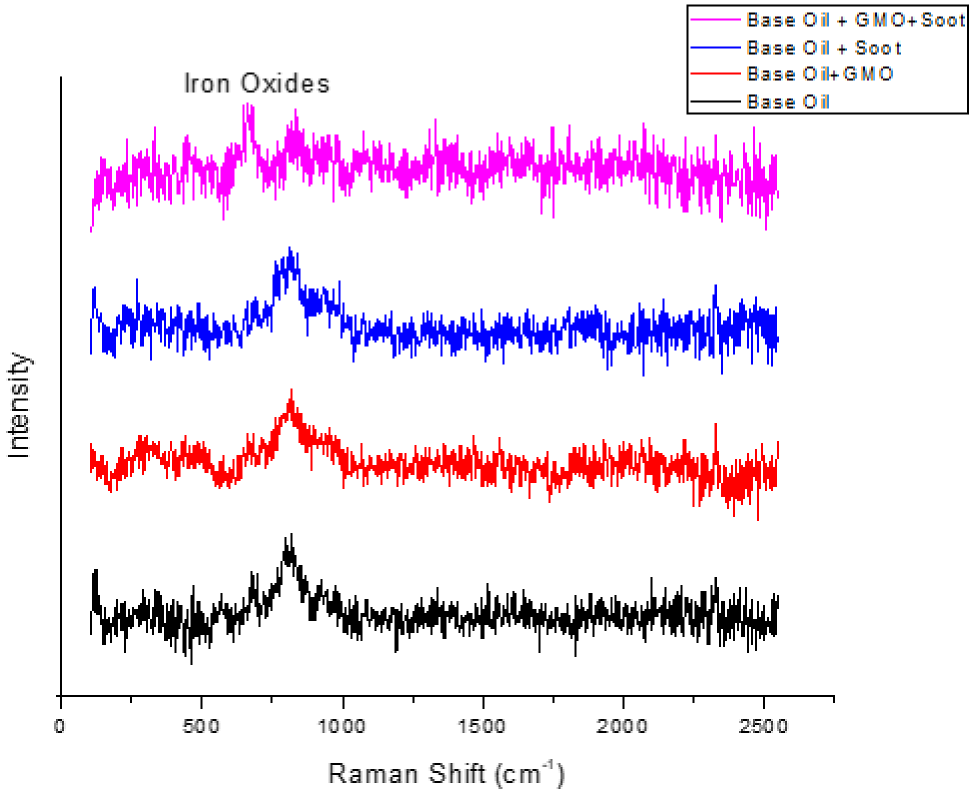

Figure 5.8. Raman Spectra taken inside the wear scar of the steel ball, after the 4 ball test for the steel on steel tribopair lubricated with all formulated lubricants

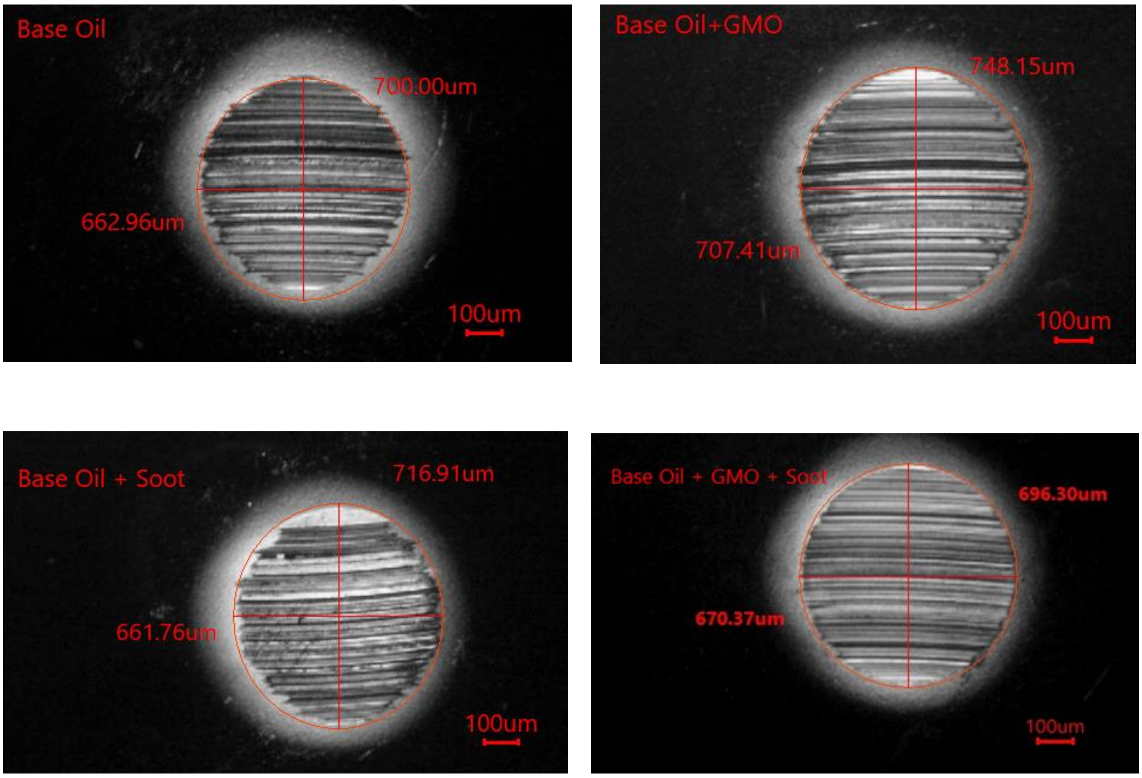

Figure 5.9. Wear scar images and measurements on steel balls obtained with an Optical Microscope fot the steel on steel tribopair lubricated in all formulated lubricants.

In Fig 5.10 b) it is shown the Raman spectra of the WDLC coating as a reference with the carbon G band appearing at around 1580 cm^{-1} and the disordered D band around 1350 cm^{-1} with an ID/IG ratio of 0.83, as well three other spectra for different spots within the wear scar of the balls coated with W-DLC using only base oil as a lubricant. In all of the spectra taken from the wear scar (Point 1, 2, 3) we can see the D peak is being more visible, and the width of the peaks are smaller, indicating the start of graphitization, the G band shifts slightly compared to the spectra of the W-DLC outside of the wear scar, indicating some changes in the coating structure, in addition ID/IG intensity ratio did not change severely (0.86) confirming small disorders of graphitized structure.[37] This indirectly means that the coating did a good job protecting against wear. This can be confirmed when we look at the wear scar in Fig 5.10 a) obtained with the optical microscope, in addition in Fig 5.11 it is shown the profile of the wear scar on the W-DLC coated ball taken with a 3D profilometer, where no noteworthy wear is visible.

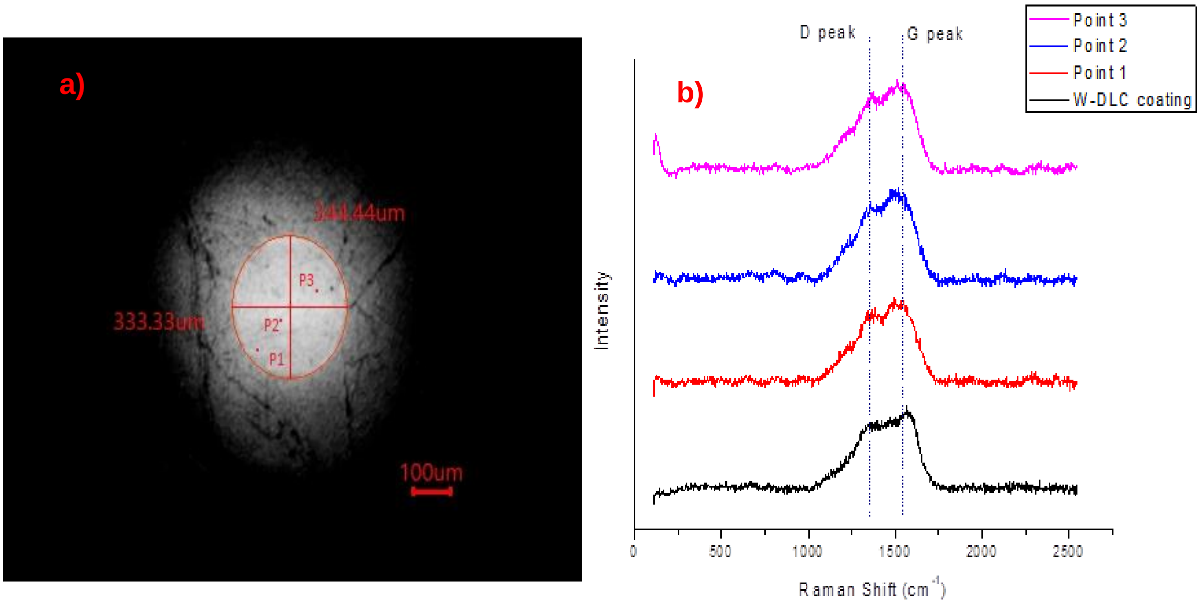

Figure 5.10. a) Wear scar image and dimensions on W-DLC coated steel ball lubricated in base oil. b) Relevant Raman Spectra taken in specified points on the wear scar image. The black spectra belonging to WDLC coating taken outside of the wear scar, it is used as a reference.

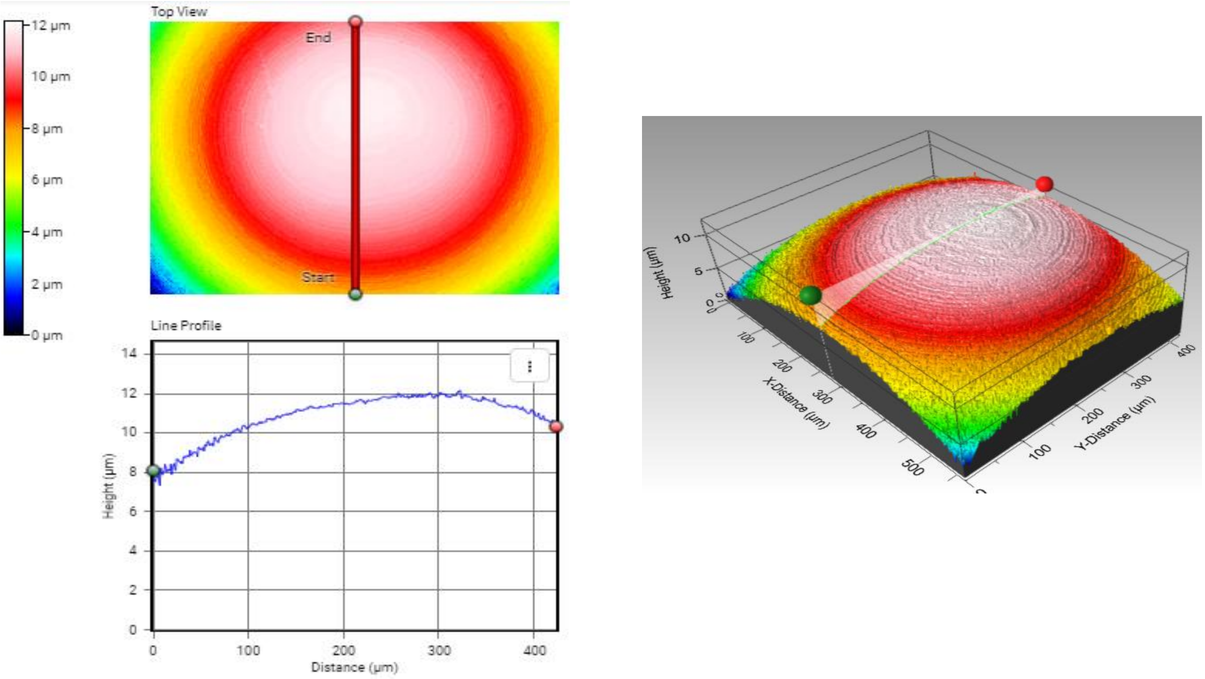

Figure 5.11. 3D profile of the wear scar on W-DLC coated steel ball lubricated in base oil

When GMO was added to the lubricant the Raman spectra (See Fig. 5.12) showed an increase of sp2 content which suggests the interaction of the carbon layer with the additive (C-C interaction), but as well as additive interaction with the coating structure (C-H interaction). The ID/IG ratio decreased to 0.59 meaning a lower degree of disorder in the graphitized structure. This agrees with other literature reported i.e., coating re-hybridization.[40] The 3D profile of the wear scar shown in Fig 5.13 does not show any wear, approving us the benefits of the coating in combination with the GMO containing lubricant.

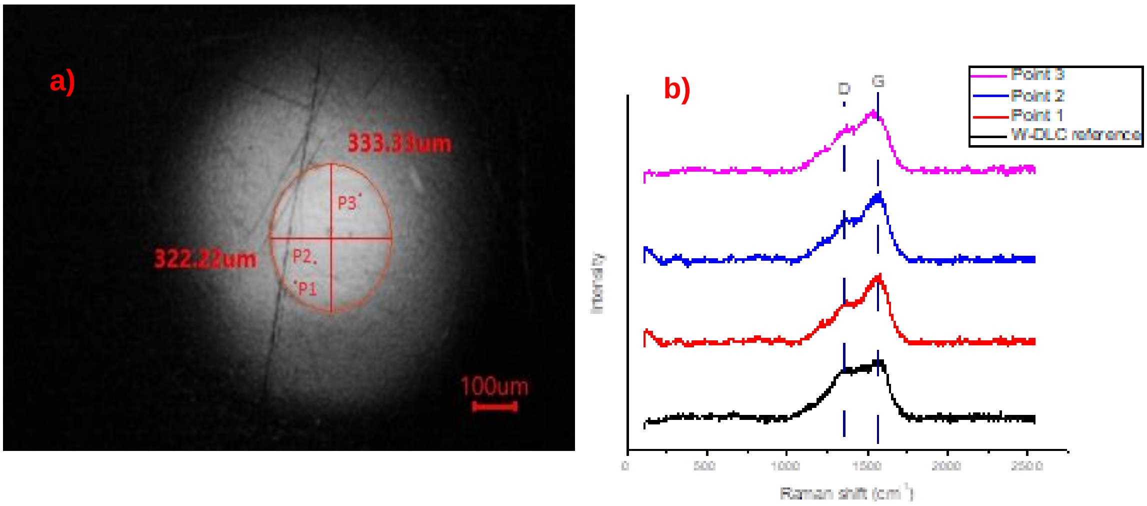

Figure 5.12 a) Wear scar image and dimensions on W-DLC coated steel ball lubricated in base oil + GMO b) Relevant Raman spectra taken in specified points on the wear scar image.

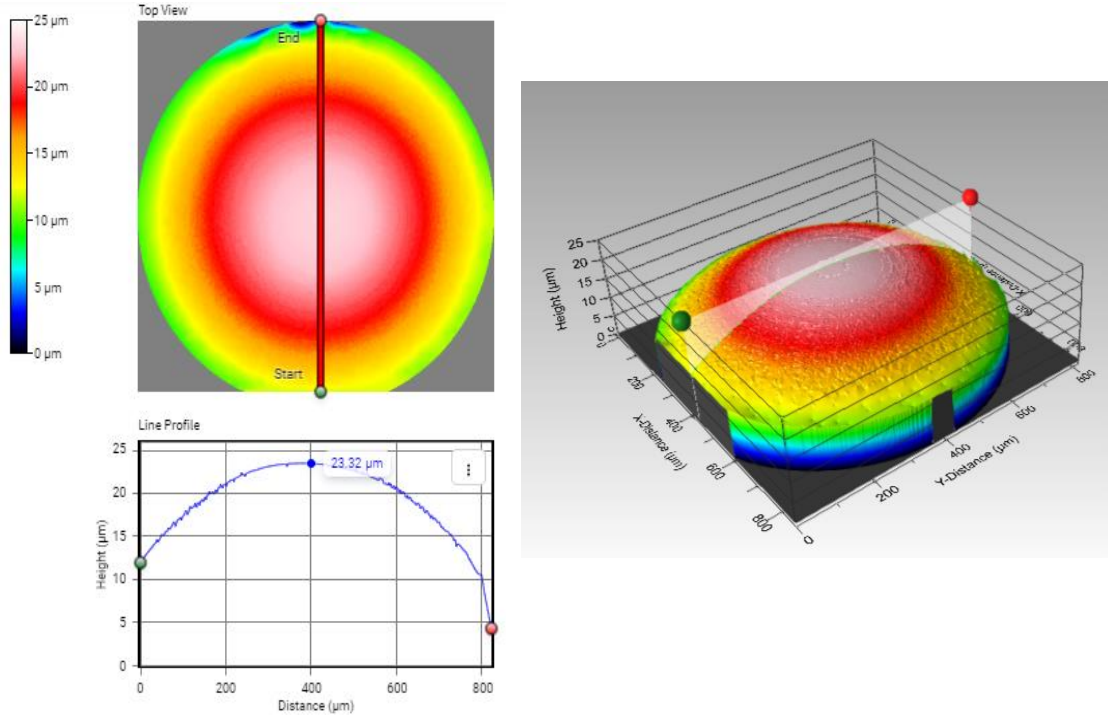

Figure 5.13 3D profile of the wear scar on W-DLC coated steel ball lubricated in base oil + GMO

Looking at Fig 5.14, visible wear started occurring when on the base oil 1% of soot was added, the Raman spectra taken in a dark place of wear scar (Point 1) shows that some spots were highly exposed and graphitized. This might have occurred because of the hard carbon black particles between the contact creating localized high-pressure areas which as a result promotes sp2 hybridization. Having a graphitic structure which is lubricious in nature explains the slightly lower friction. The location of Point 1 showed us as well that the coating material was transferred and agglomerated in some parts of the wear scar acting as a solid lubricant. The structure of the coating here is more crystalline.

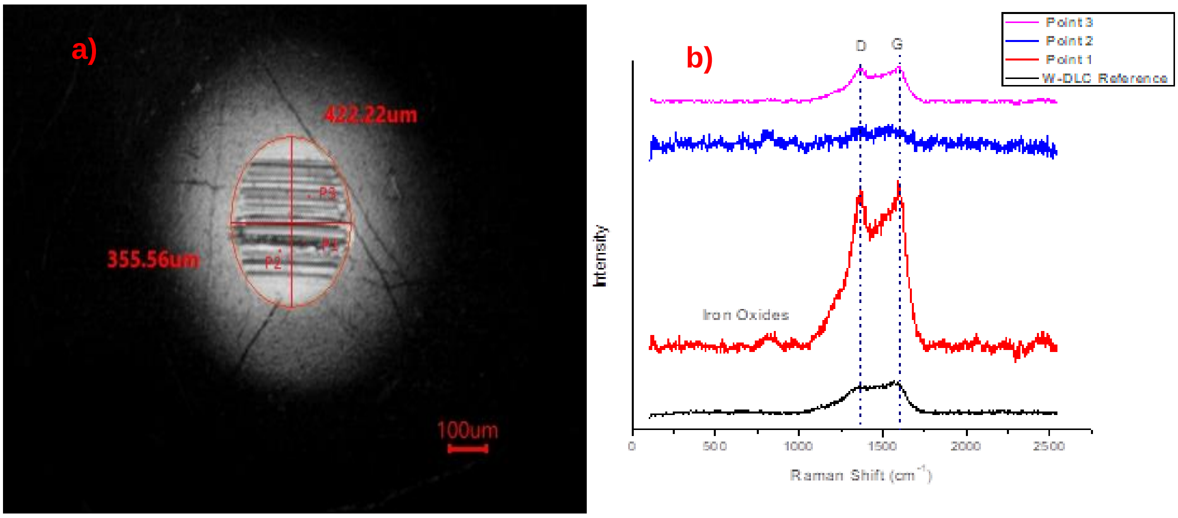

Figure 5.14. a) Wear scar image and dimensions on W-DLC coated steel ball lubricated in base oil + soot b) Relevant Raman Spectra taken in specified points on the wear scar image.

In addition, peaks raising around 690 and 817 cm^{-1} are due to v(O-W-O) stretching vibrations that are characteristics of h-WO_3. Those bends are broadened because of the nanocrystalline nature of h-WO_3 films.[41] Point 2 shows just a very low intensity of D and G peaks, apparently the spectra obtained here is mostly from the substrate.

The Raman spectra in Point 3 (Gray Surface) confirms that there is still coating present, because of the shift of the G peak and the increase of the intensity of the D peak graphitization has occurred. The 3D profile (See Fig 5.15) of this sample shows the depth of the wear scar, confirming that the wear in some places was deep enough to exceeding the 1730 nm coating thickness.

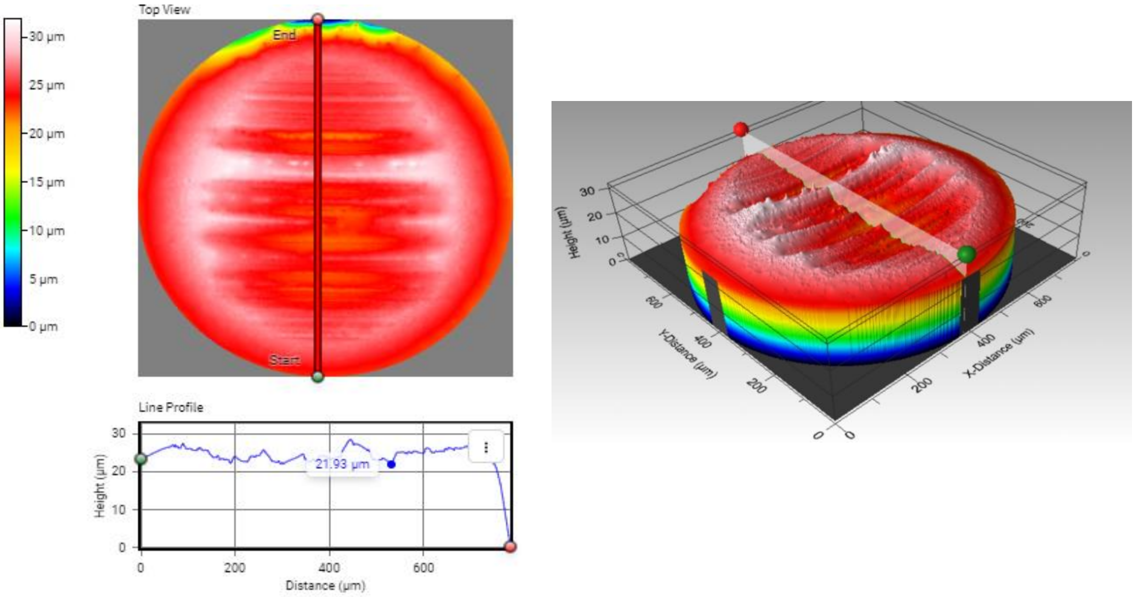

Figure 5.15 3D profile of the wear scar on W-DLC coated steel ball lubricated in base oil + soot

When GMO is added in the lubricant containing soot, we observed that it made a difference, apparently GMO suppresses the interaction of soot with the surface by creating a thin tribofilm in between. In previous studies it was confirmed using SIMS analyses the formation of a thin tribofilm of the size of 2nm when GMO is added in a system where DLC is present. Supposedly the degradation of GMO will produce OH species on the surface of carbon, particularly by the reaction with the carbon radical. The adsorption of mono-molecular layer in the DLC surface is schematically shown in Fig. 5.16. For a fundamental study of the tribochemistry of the surface with the additive, EELS as a semi-quantitative method are recommended. [42]

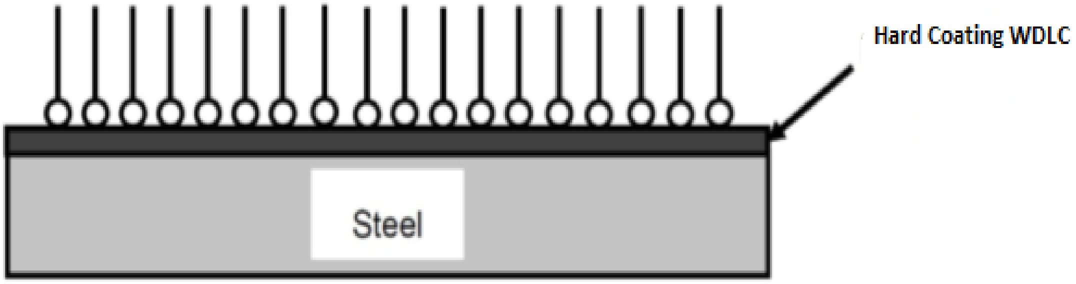

Figure 5.16 Schematic representation of the adsorption of mono-molecular layer in the DLC surface

The Raman spectra's in Fig. 5.17 taken in three different points of the wear scar show the same trendline. The G peak does not show any shift, indicating no change in the structure of the coating. No oxidation peaks are observed. The good performance of the coating in combination with the lubricant here is confirmed as well by the 3D profile of the wear scar as shown in Fig.5.18

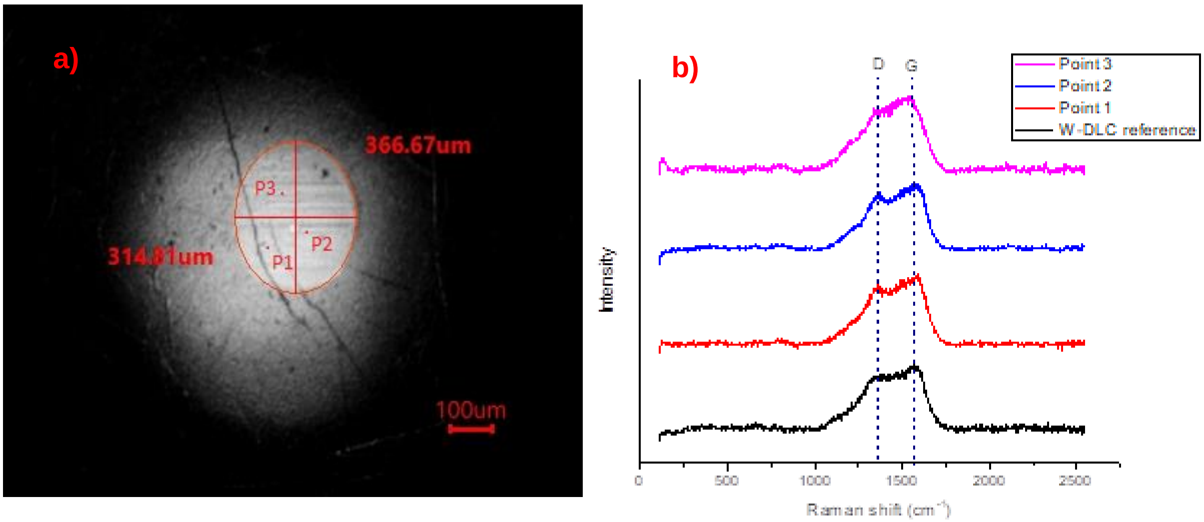

Figure 5.17 a) Wear scar image and dimensions on W-DLC coated steel ball lubricated in base oil + soot + GMO b) Relevant Raman Spectra taken in specified points on the wear scar image.

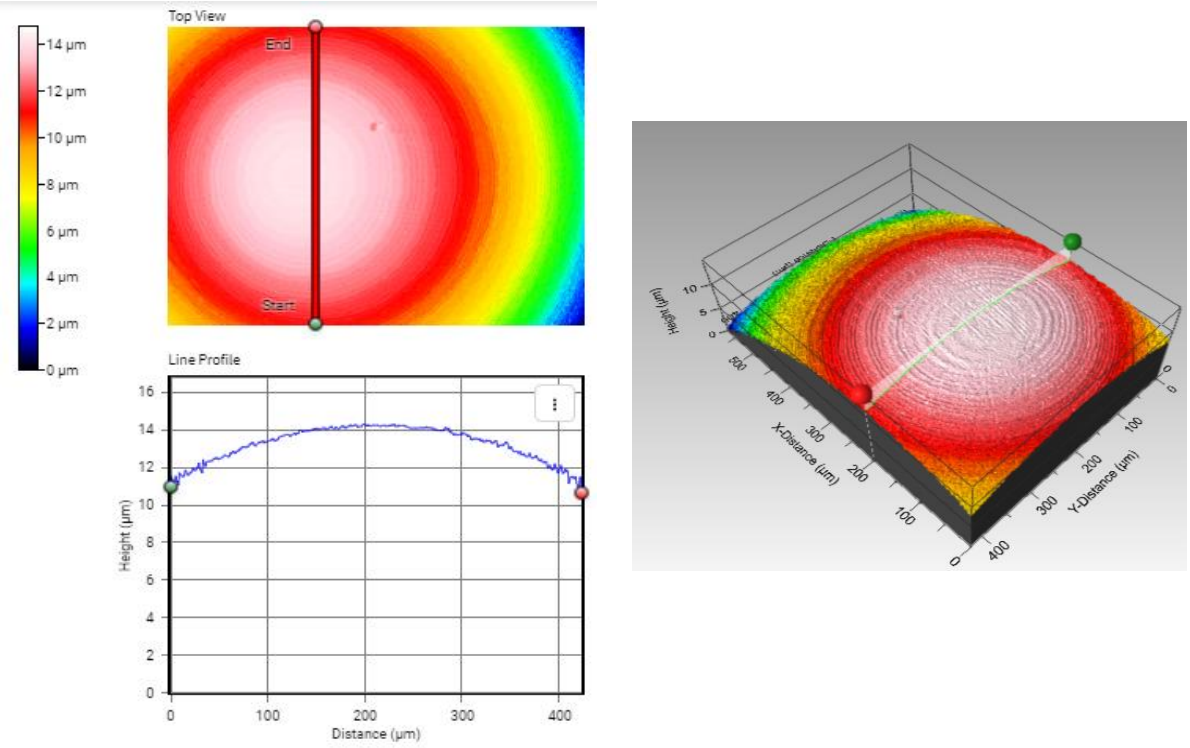

Figure 5.18 3D profile of the wear scar on W-DLC coated steel ball lubricated in base oil + soot + GMO

5.3 Ag-DLC

5.3.1 Friction evaluation

As attached in Annex C the results of friction coefficient of Steel against Ag-DLC lubricated in formulated oils do not show any noticeable changes when compared between the lubricants used, but if we compare the COF between steel on Ag-DLC contact and steel on steel we can see that the first one shows a lower COF. This can be attributed to the coating and the graphitization of the coating structure as shown later in this report. The same did not apply for the last case where soot and GMO where present in the base oil, here the COF for the steel on Ag-DLC was higher than the one for steel on steel, although the last one showed a lot of fluctuation.

5.3.2 Wear Results

According to the mean wear scar graph (See Annex C) and the 3D profile taken on all the sample balls (Annex D) we can see the difference on the wear according to the lubricant we used. Initially Ag-DLC coatings showed more wear compared to steel when lubricated on base oil only. This change after adding GMO where the wear scar decreased noticeably. The effect of soot in this system could be noticed as well, we had more wear compared with the soot free, GMO containing lubricant. Result of the wear scar diameter in Annex C showed that the wear scar decreased in the case when the lubricant contained soot, compared to the system where the tribopair was lubricated only in base oil. This might have happened because of silvers ability to agglomerate on the surface and with it being an inert material it might have repealed the soot. To prove this SEM and EDS analyses need to be done. Introducing GMO in the case where soot was already involved benefited the situation even more. As GMO is known to be very reactive to carbon it might have reacted with the soot particles and in cooperation with the inert silver decreased the wear even further.

5.3.3 Raman results

In order to evaluate the importance of silver on the carbon structure while operating in boundary lubrication conditions, Raman spectroscopy was performed. As shown in the graphs included in Annex D the Raman spectum of the coating itself shows the typical D and G peaks located around 1350 cm^{-1} and1550 cm^{-1}.[43] When the coating was tested in base oil visible wear was observed (See optical image of the wear scar included in Annex D). The coating during the contact with the counter body gathered on the wear scar, Raman spectra on the black parts shows intense D and G peaks. We can notice that the G peak is positioned in a higher wavenumber, intending an increase of graphite like bonds. On the other hand, the bright parts of the coating show almost no D and G peak, therefore iron oxide peaks from the substrate are visible around 600 to 800 cm^{-1}.

When GMO was introduced the peaks of Iron Oxides found on the bright parts of the wear scar increased in intensity, while in the dark parts coating still was present as the D and G peaks where found. The ID/IG ratio decreased to 0.61 showing less defects on the structure compared only to base oil lubricated system with an ID/IG ratio of 0.816. When soot was added to base oil the ID/IG ratio (0.810) of the D and G peaks found in the dark part of the wear scar was almost the same with the one obtained when the test was performed only with base oil.

When a combination of 1% of soot and 1% of GMO where added to the base oil in most parts of the wear scar intense D and G peaks where found, meaning that the coating was present in most parts of the wear scar, the ID/IG ratio (0.90) was higher than the one obtained only with base oil and the G peak in all spectra taken showed a shift to a higher wavenumber, giving us all primary factors for the creation of a graphitization layer, indicating less wear.

To have a more detailed analyses of the chemistry in between the tribo-couple, other characterization techniques could be useful to further investigate the formation of silver-based compounds and in addition their role on the tribological properties of the coating.

6. Conclusion

From the above results, we can conclude that:

- Steel against DLC showed better wear and friction results compared to a DLC/DLC contact and is economically more favorable.
- W-DLC showed lower coefficient of friction and lower wear compared to steel when lubricated in base oil, proving the benefits of the coating.
- Steel/W-DLC showed lower wear and coefficient of friction compared to steel/steel contact for all formulated lubricants.
- W-DLC showed lower wear and coefficient of friction and wear compared to Ag-DLC for all formulated lubricants.
- Soot has only minor impact in the W-DLC coating when it is present in the base oil, it tends to change the coating structure and initiate graphitization
- When GMO is added soot seems to have no impact on the coating wear
- Ag-DLC coatings tended to repeal soot, better results were obtained then steel/steel contact but worse if compared to W-DLC

7. Future oil analyses

It is expected that lubricants will undergo an Oxidation and Total Acid Number Test (TAN) performed in a lab in New York, USA, for better evaluation and understanding of the impact of W-DLC, Ag-DLC and GMO in soot wear, so further developments for soot wear resistant lubricants and coatings can be done.

References

[1] Market Research. (2017). *Automotive Manufacturing Industry to Reach 1.7 Trillion by 2015*. [online] Available at: http://MarketResearch.com

[2] Washington Times. (n.d.). *EPA locks fuel economy standards through 2025*.

[3] *Rapid Testing of Automotive Components at Very High Temperatures*, (2017). [Webinar] Bruker Tribology Webinar.

[4] Kapoor, A., Schwartz, S., Priest, M. and Dwyer-Joyce, R. (2000). *Automotive Tribology" in "Modern Tribology Handbook"*. CRC Press LLC.

[5] Jost Report (1966), *HMSO, Lubrication, Tribology, Education and Research*, DES Report, London, UK.

[6] Science, K. and Science, I. (n.d.). *What is Friction?*. [online] Face-kyowa.co.jp. Available at: https://www.face-kyowa.co.jp/english/en_science/en_what_friction.html [Accessed 13 Jul. 2019].

[7] Encyclopedia Britannica. (2019). *Wear | physics*. [online] Available at: https://www.britannica.com/science/wear [Accessed 13 Jul. 2019].

[8] Parker, D.A. and Adams, D.R. (1982), *Friction losses in the reciprocating internal combustion engine*, I. Mech E Conference, Paper no. C5/82

.

[9] F. Motamen Salehi, D.N. Khaemba, A. Morina, A. Neville, Corrosive–Abrasive Wear Induced by Soot in Boundary Lubrication Regime, Tribol. Lett. 63 (2016) 1–11. doi:10.1007/s11249-016-0704-9.

[10] Olomolehin, Y., Kapadia, R., Spikes, H. (2010), *Antagonistic interaction of antiwear additives and carbon black.* Tribol. Lett. 37(1), 49–58. doi:10.1007/s11249-009-9489-4

[11] Holmberg K, Andersson P, Erdemir A. (2012), *Global energy consumption due to friction in passenger cars.* Tribol Int 47: 221–234

[12] Holmberg K., Andersson P, Nylund O, Mäkelä K. (2014) *Global energy consumption due to friction in trucks and buses*. Tribol Int 78: 94–114

[14] Lubrizol Additives 360. (2011). *How Soot in Engine Oil Affects Wear*. [online] Available at: http://lubrizoladditives360.com/soot-engine-oil-affects-wear

[13] Holmberg, K. and Erdemir, A. (2017). Influence of tribology on global energy consumption, costs and emissions. *Friction*, 5(3), pp.263-284.

[15] Bishop, I.N. (1964), *Effect of design variables on friction and economy*, SAE Paper 812A.

[16] Ku, Y. and Patterson, D. (1988), *Piston and ring friction by the fixed sleeve method*, SAE 880571.

[17] Basshuysen, Richard van Schäfer, Fred. (2016). *Internal Combustion Engine Handbook - Basics, Components, System, and Perspectives (2nd Edition).* SAE International.Retrieved from https://app.knovel.com/hotlink/toc/id:kpICEHBC04/internal-combustion-engine/internal-combustion-engine

[18] Machinerylubrication.com. (n.d.). *Base Oil Groups Explained*. [online] Available at: https://www.machinerylubrication.com/Read/29113/base-oil-groups [Accessed 13 Jul. 2019].

[19] Chemceed. (n.d). *Advantages of Synthetic Ester Base Stocks - Chemceed*. [online] Available at: https://www.chemceed.com/product-news/advantages-synthetic-ester-base-stocks/ [Accessed 13 Jul. 2019].

[20] Ihsmarkit.com. (n.d). *Lubricating Oil Additives - Specialty Chemicals Update Program (SCUP) | IHS Markit*. [online] Available at: https://ihsmarkit.com/products/chemical-lubricating-oil-scup.html [Accessed 13 Jul. 2019].

[21] Infineuminsight.com. (2017). *Additive Components*. [online] Available at: https://www.infineuminsight.com/media/1802/7-additive-components-v4a.pdf [Accessed 13 Jul. 2019].

[22] Green, D. (2015). *The tribological effect of soot contaminated lubricants on engine components.* Ph.D. University of Sheffield.

[23] Robertson, J. (2002). *Diamond-like amorphous carbon. Materials Science and Engineering: R: Reports*, 37(4-6), pp.129-281.

[24] HIPIMS technology. (n.d.). *DLC Coatings - Diamond-Like Carbon Coatings*. [online] Available at: http://www.richterprecision.com [Accessed 31 Jan. 2019].

[25] Wasy, A.; Balakrishnan, G.; Lee, S.; Kim, J.-K.; Kim, T. G.; Song, J. I. (2015). "*Thickness dependent properties of diamond-like carbon coatings by filtered cathodic vacuum arc deposition". Surface Engineering*. **31** (2): 85–89. doi:10.1179/1743294414Y.0000000254.

[26] Manninen, N., Ribeiro, F., Escudeiro, A., Polcar, T., Carvalho, S. and Cavaleiro, A. (2013). I*nfluence of Ag content on mechanical and tribological behavior of DLC coatings. Surface and Coatings Technology*, 232, pp.440-446.

[27] Zahid, R., Haji Hassan, M., Alabdulkarem, A., Varman, M., Mufti, R., Kalam, M., Binti Mohd Zulkifli, N., Gulzar, M. and Lee, T. (2017). Investigation of the tribochemical interactions of a tungsten-doped diamond-like carbon coating (W-DLC) with modeled palm trimethylolpropane ester (TMP) and polyalphaolefin (PAO). *RSC Advances*, 7(43), pp.26513-26531.

[28] Nhbb.com. (n.d.). *Hard Coatings – Diamond-like Carbon and Tungsten Carbon Carbide*. [online] Available at: https://nhbb.com/reference/mini-instrument-bearings/hard-coatings.aspx [Accessed 13 Jul. 2019].

[29] Yu, X., Qin, Y., B Wang, C., Q Yang, Y. and X Ma, C. (2013). *Vacuum*. pp.82-85.

[30] Wu, Y., Chen, J., Li, H., Ji, L., Ye, Y. and Zhou, H. (2019). *Preparation and properties of Ag/DLC nanocomposite films fabricated by unbalanced magnetron sputtering*.

[31] Ducom Instruments - The Tribology Company. (n.d.). *Four Ball Tester | Ducom Instruments - The Tribology Company*. [online] Available at: http://ducom.com/test-instruments/lubricant-testers/four-ball-tester/

[33] Angstromsciences.com. (n.d.). *Magnetron Sputtering Deposition – magnetron sputtered thin films*. [online] Available at: https://www.angstromsciences.com/magnetron-sputtering-deposition

[34] Di Gianfrancesco, A. (2017). Technologies for chemical analyses, microstructural and inspection investigations. *Materials for Ultra-Supercritical and Advanced Ultra-Supercritical Power Plants*, pp.197-245.

[35] Nanoscience Instruments. (n.d.). *Optical Profilometry - Nanoscience Instruments*. [online] Available at: https://www.nanoscience.com/techniques/optical-profilometry/ [Accessed 13 Jul. 2019].

[36] Princton Instruments. (2019). *Raman Spectroscopy Basics*. [online] Available at: http://web.pdx.edu/~larosaa/Applied_Optics_464-564/Projects_Optics/Raman_Spectrocopy/Raman_Spectroscopy_Basics_PRINCETON-INSTRUMENTS.pdf [Accessed 13 Jul. 2019].

[37] Yang, L., Neville, A., Brown, A., Ransom, P. and Morina, A. (2014). Friction reduction mechanisms in boundary lubricated W-doped DLC coatings. *Tribology International*, 70, pp.26-

[38] Lu, J. and Tsai, C. (2014). Hydrothermal phase transformation of hematite to magnetite. *Nanoscale Research Letters*, 9(1).

[39] Merz, R., Brodyanski, A. and Kopnarski, M. (2015). On the Role of Oxidation in Tribological Contacts under Environmental Conditions. *Conference Papers in Science*, 2015, pp.1-11.

[40] Yang, L., Neville, A., Brown, A., Ransom, P. and Morina, A. (2015). Effect of Lubricant Additives on the WDLC Coating Structure When Tested in Boundary Lubrication Regime. *Tribology Letters*, 57(2).

[41] Djaoued, Y., Balaji, S. and Brüning, R. (2012). Electrochromic Devices Based on Porous Tungsten Oxide Thin Films. *Journal of Nanomaterials*, 2012, pp.1-9.

[42] Yazawa, S., Minami, I. and Prakash, B. (2014). Reducing Friction and Wear of Tribological Systems through Hybrid Tribofilm Consisting of Coating and Lubricants. *Lubricants*, 2(2), pp.90-112.

[43] Manninen, N., Ribeiro, F., Escudeiro, A., Polcar, T., Carvalho, S. and Cavaleiro, A. (2013). Influence of Ag content on mechanical and tribological behavior of DLC coatings. *Surface and Coatings Technology*, 232, pp.440-446.

Annex A – Base Oil and Additive Specifications

Base oil	Manufacturer	City and country
Radialube 7250	**Oleon**	**Oelegem, Belgium**

Result of analyses	Unit	Results	Min.	Max.	Method
Acid Value	**mg KOH/g**	**0.03**	**0.00**	**0.10**	**AOCS Cd 3d-63**
Iodine Value	**g I2/100g**	**2.9**	**0.0**	**7.0**	**Oleon OA-020**
Water	**%(m/m)**	**0.05**	**0.00**	**0.05**	**AOCS Ca 2e-84**
Gardner		**2.30**	**0.00**	**6.00**	**AOCS Td 1a-64**
Viscosity 40^{o}**C**	**cST**	**96.7**	**91.0**	**97.0**	**ASTM D445**
Ti+Si	**ppm**	**0.5**	**0.5**	**5.0**	**Oleon OS-074**
Pour Point	^{o}C	**-43**	**-43**	**-30**	**ASTM D97**

Additive	Manufacturer	City and country
Radiasurf 7150 GMO	**Oleon**	**Oelegem, Belgium**

Result of Analyses	Unit	Results	Min.	Max.	Method
Acid Value	**mg KOH/g**	**0.18**	**0.00**	**1.00**	**AOCS Cd 3d-63**
Iodine Value	**g I2/100g**	**79.6**	**75.0**	**81.0**	**Oleon OA-020**
Saponification Value	**mg KOH/g**	**167.9**	**166.0**	**175.0**	**AOCS Cd 3-25**
Alpha-Monoglycerides	**%(m/m)**	**42.8**	**40.0**	**50.0**	**AOCS Cd 11-57**
Free Glycerol Content	**%(m/m)**	**1.60**	**0.00**	**2.00**	**AOCS Ca 14-56**
Water	**%(m/m)**	**0.01**	**0.00**	**0.50**	**AOCS Ca 2e-84**
Cloud Point	^{o}C	**7.4**	**-10.0**	**10.0**	**AOCS Cc 6-25**
Lovibond 1”, Yellow		**3.4**	**0.0**	**15.0**	**AOCS Cc 13b-45**
Lovibond 1”, Red		**1.0**	**0.0**	**3.0**	**AOCS Cc 13b-45**

Annex B-Coefficient of friction for Steel/W-DLC contact lubricated in the formulated lubricants

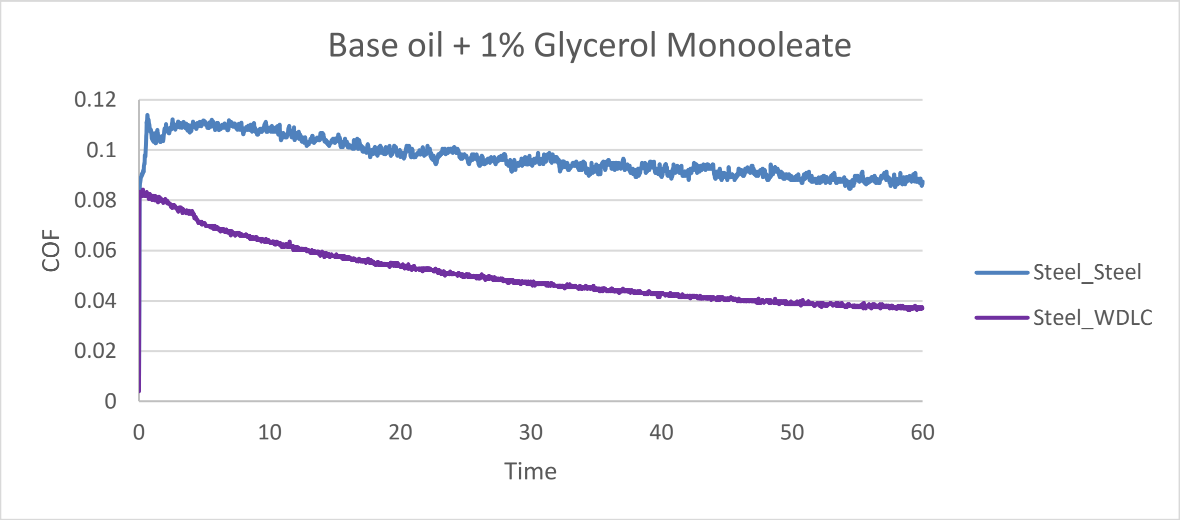

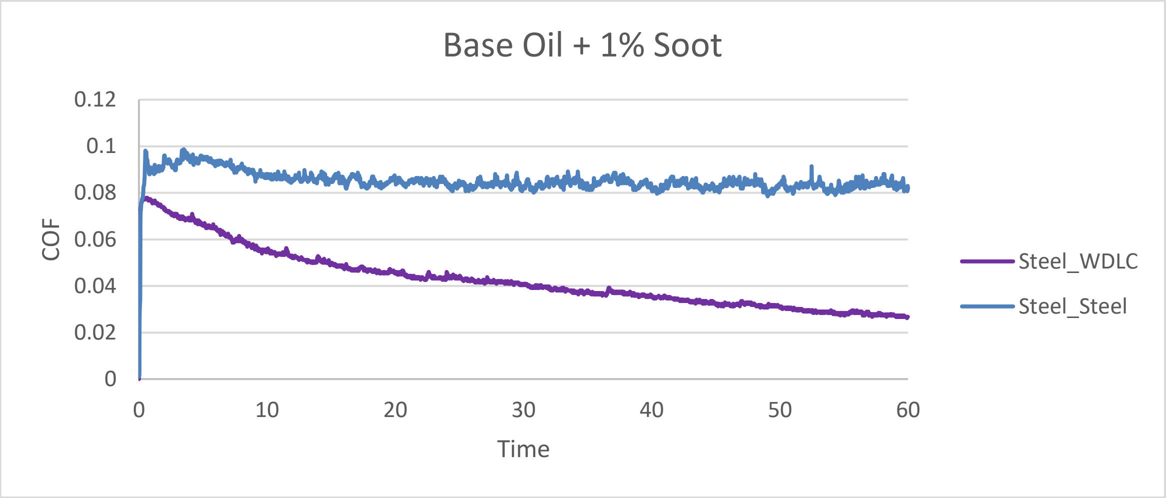

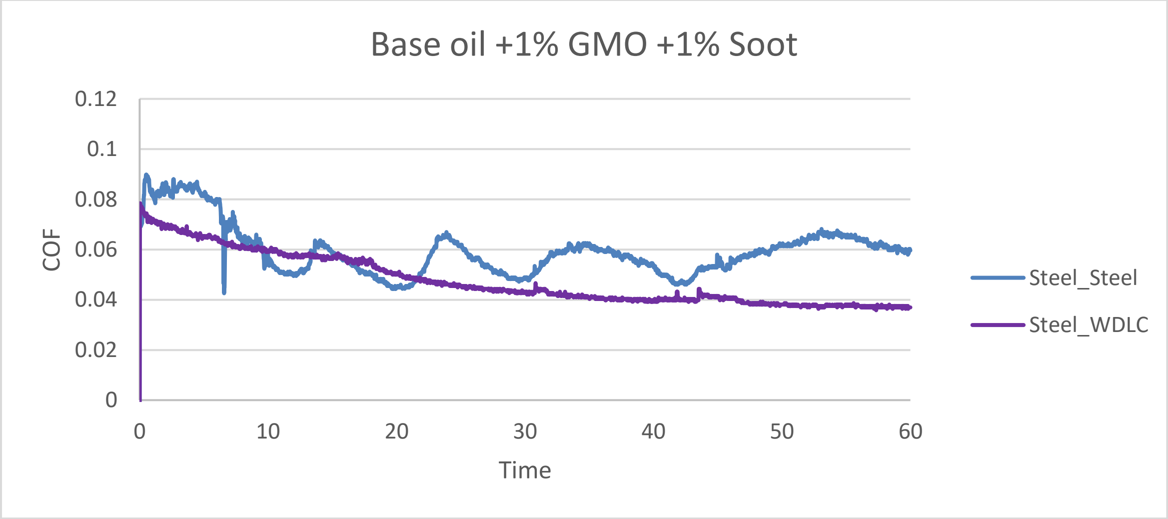

Annex C –Coefficient of friction and mean wear scar diameter for Steel/Ag-DLC contact lubricated in all formulated lubricants

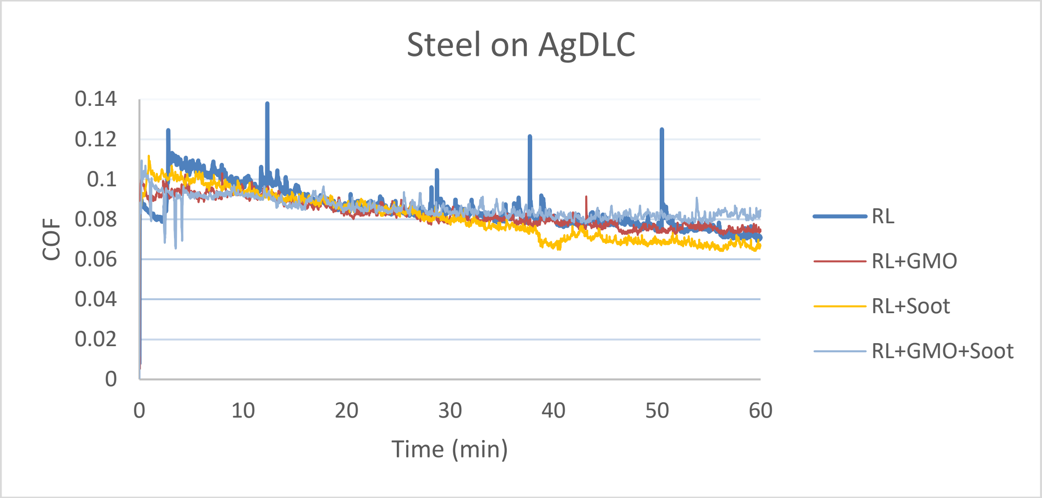

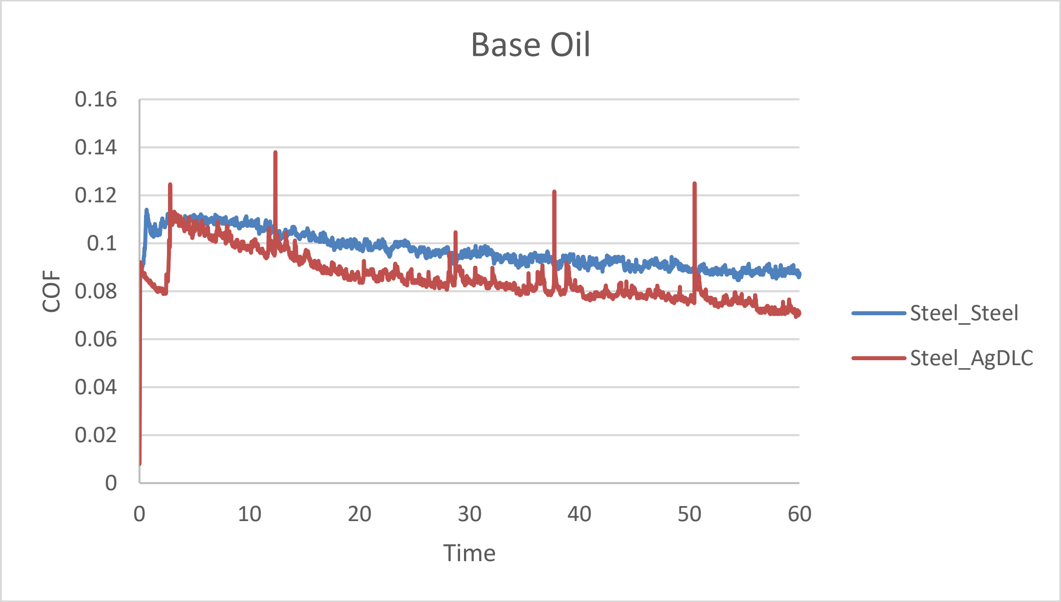

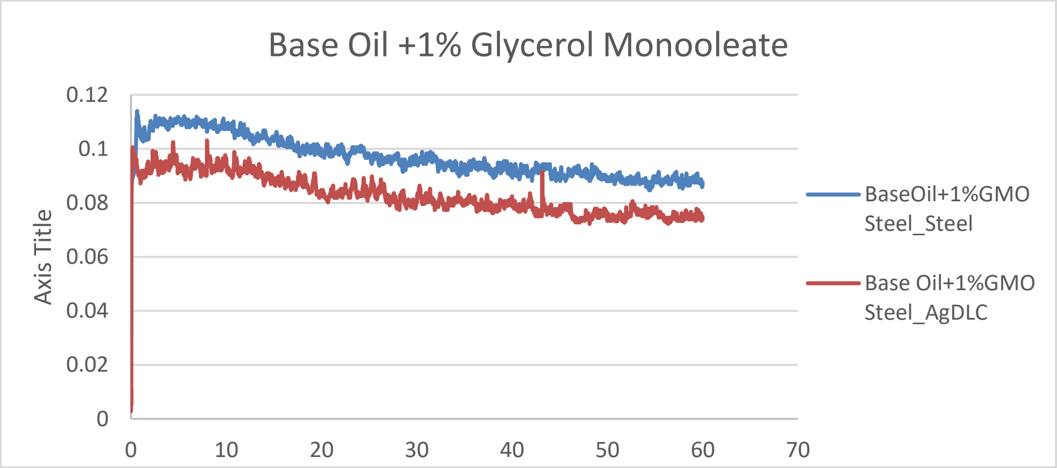

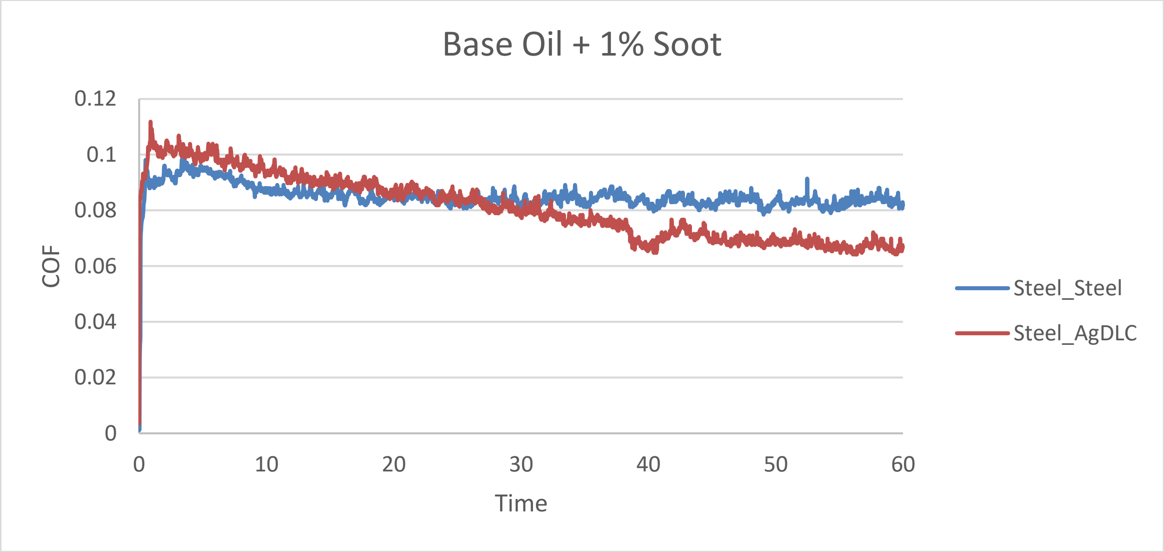
Base Oil + 1% Soot
COF
0.12
0.1
0.08
0.06
0.04
0.02
0
0
10
20
30
40
50
60
Time
Steel_Steel
Steel_AgDLC

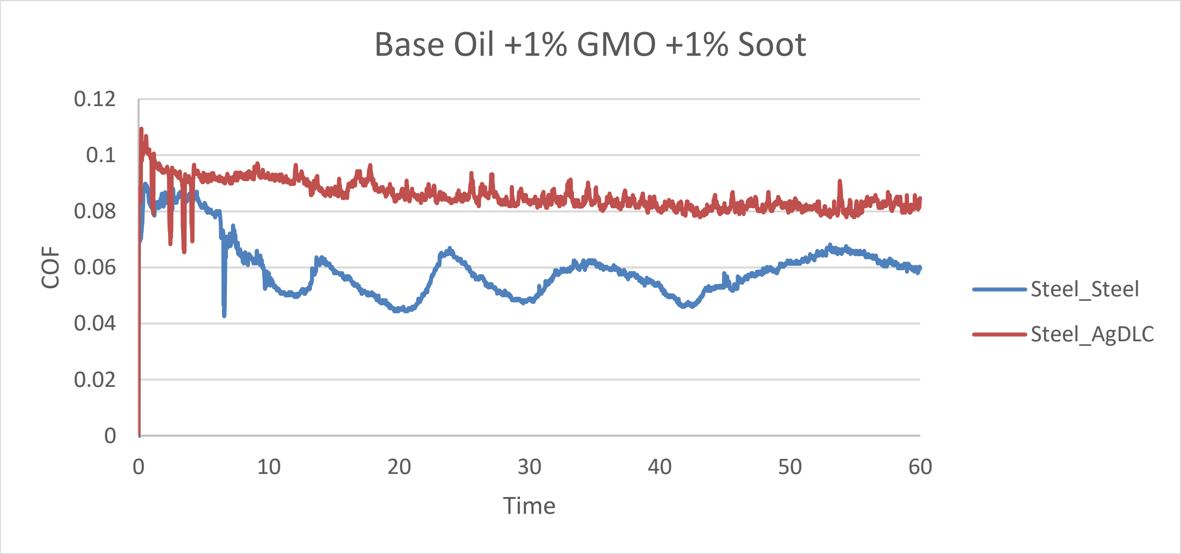
Base Oil +1% GMO +1% Soot
COF
0.12
0.1
0.08
0.06
0.04
0.02
0
0
10
20
30
40
50
60
Time
Steel_Steel
Steel_AgDLC

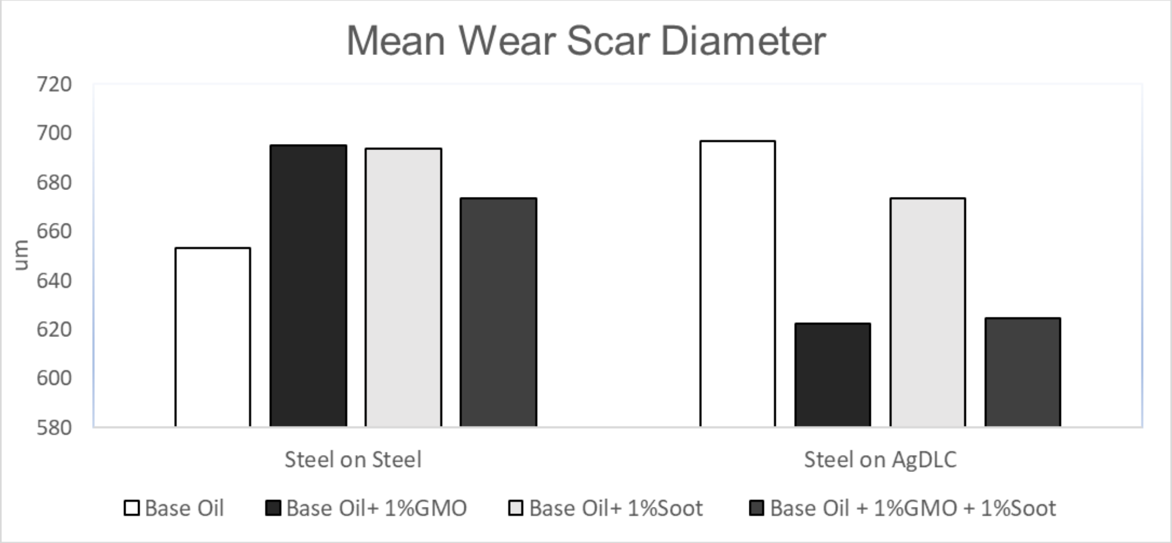
Mean Wear Scar Diameter
um
720
700
680
660
640
620
600
580
Steel on Steel
Steel on AgDLC
Base Oil
Base Oil+ 1%GMO
Base Oil+ 1%Soot
Base Oil + 1%GMO + 1%Soot

Annex D – Wear images, Raman spectroscopy and 3D profile of Ag-DLC Wear Scars

Base Oil

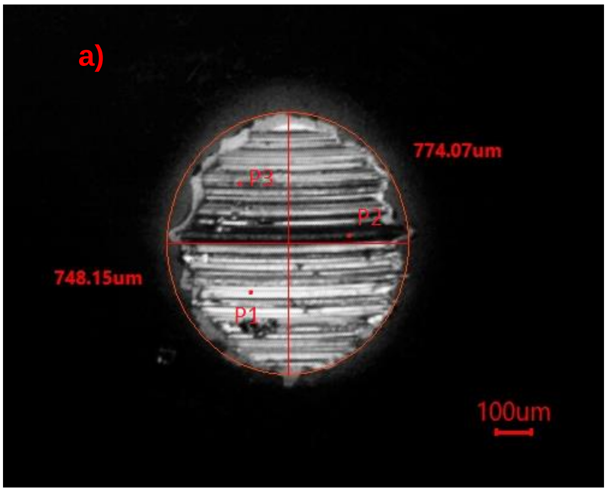

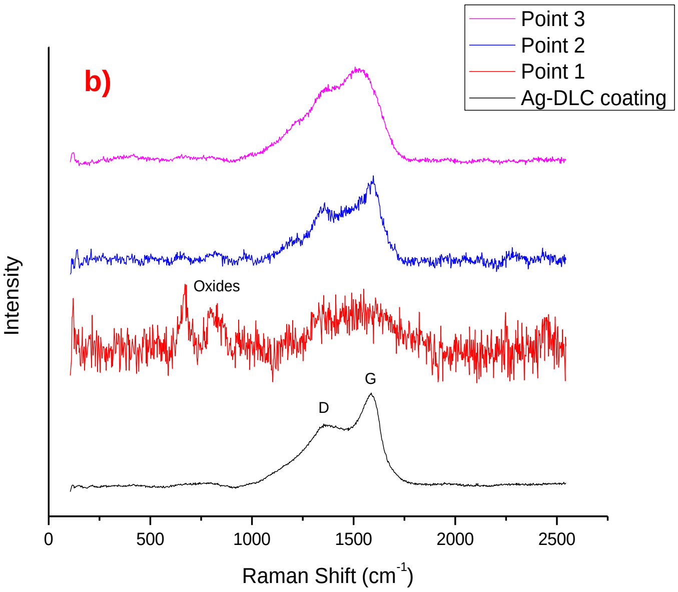

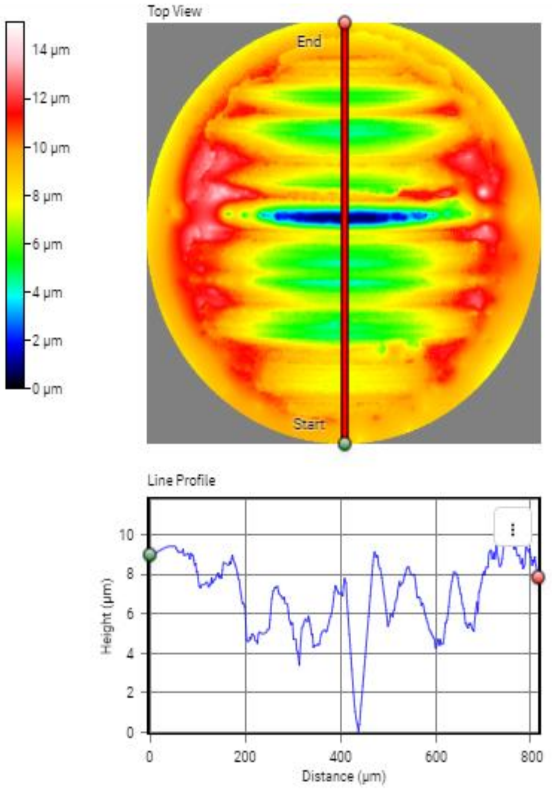

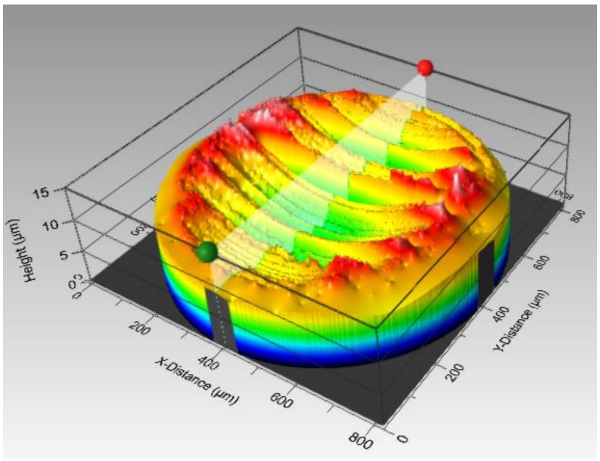

Base Oil + GMO

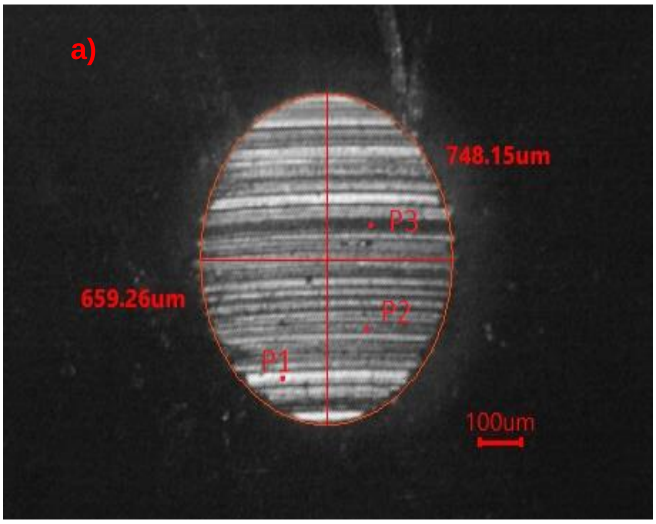
a)
748.15um
P3
659.26um
P2
P1
100um

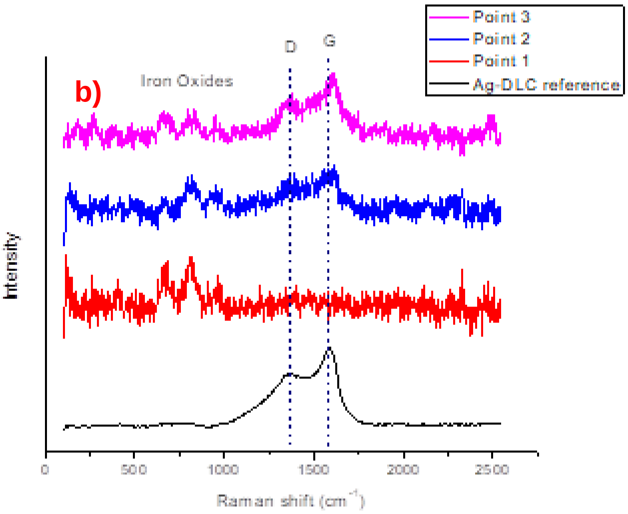
b)
Point 3
Point 2
Point 1
Ag-DLC reference
D
G
Iron Oxides
Intensity
0
500
1000
1500
2000
2500
Raman shift (cm^{-1})

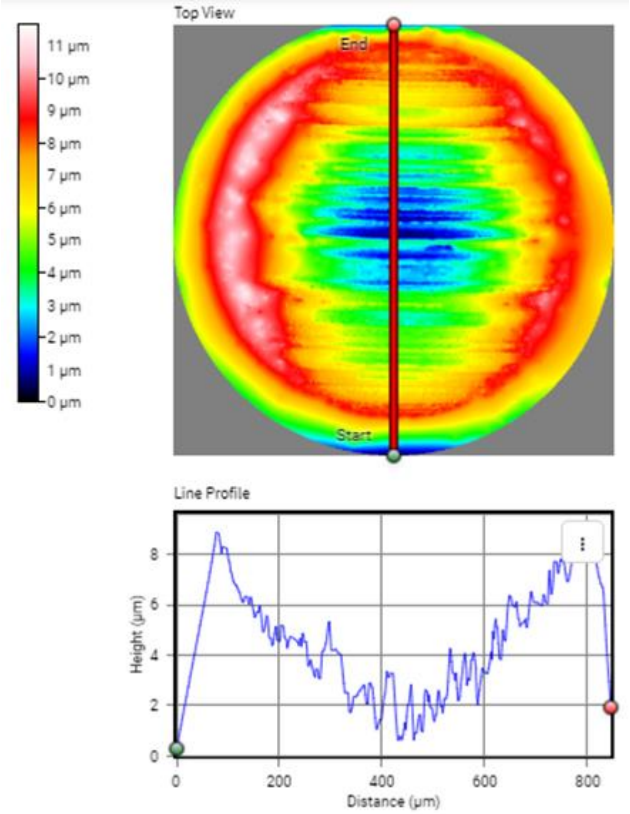
Top View
11 µm
10 µm
9 µm
8 µm
7 µm
6 µm
5 µm
4 µm
3 µm
2 µm
1 µm
0 µm
End
Start
Line Profile
Height (µm)
8
6
4
2
0
0
200
400
600
800
Distance (µm)

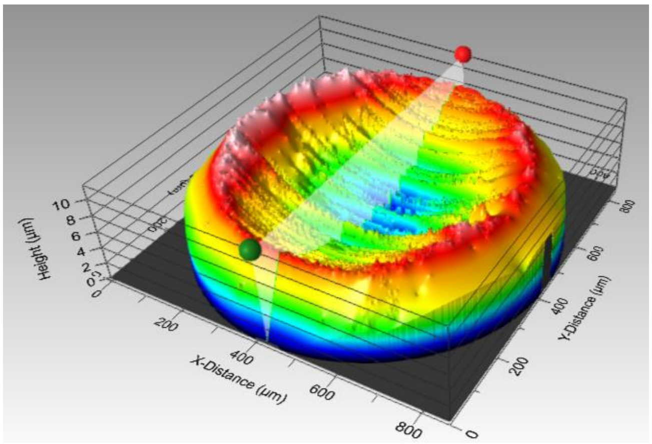
Height (µm)
10
8
6
4
2
0
200
400
600
800
X-Distance (µm)
0
200
400
600
800
Y-Distance (µm)

Base Oil + Soot

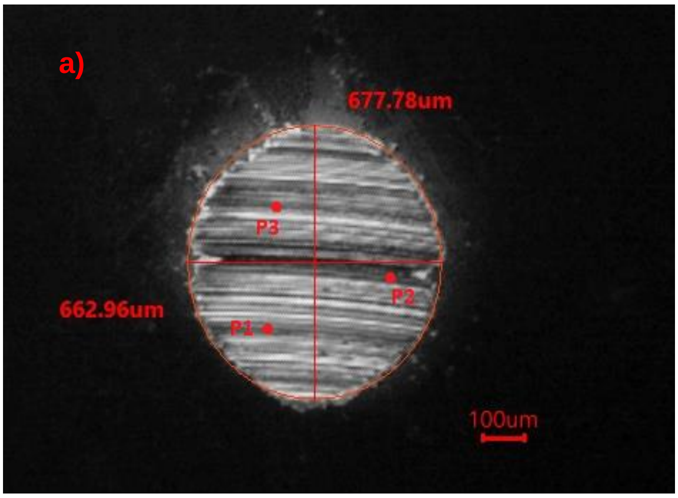

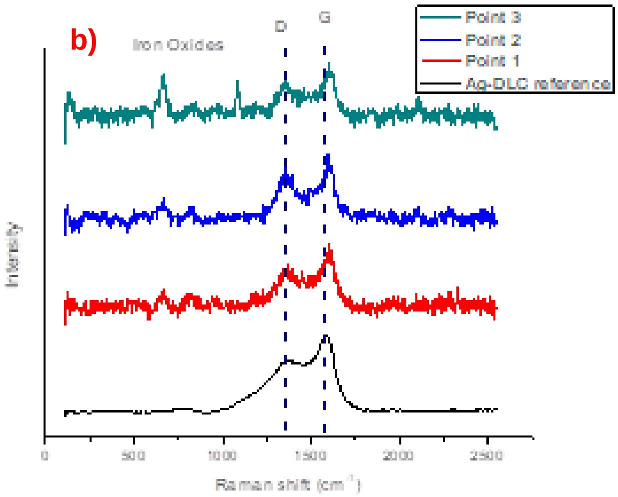

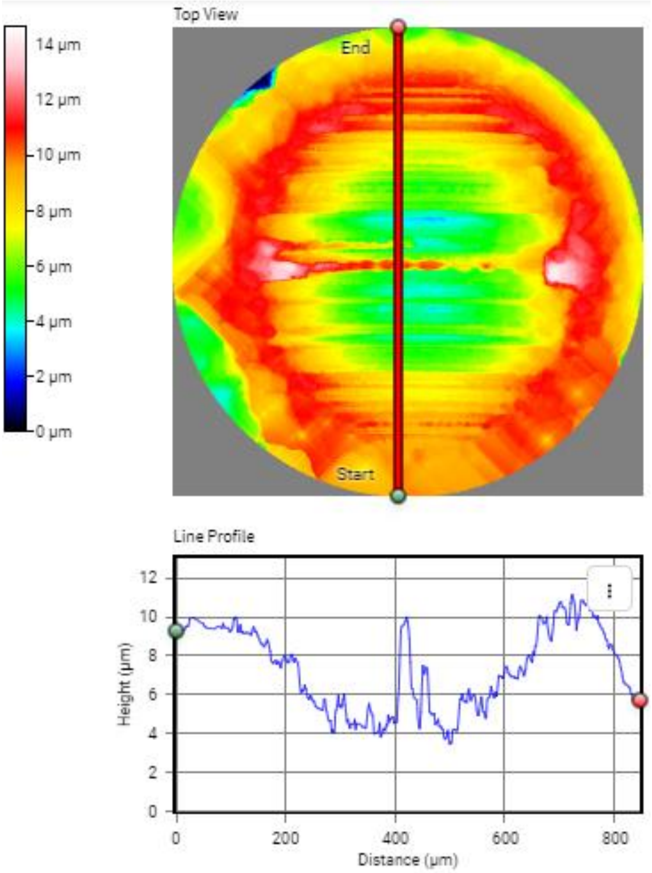

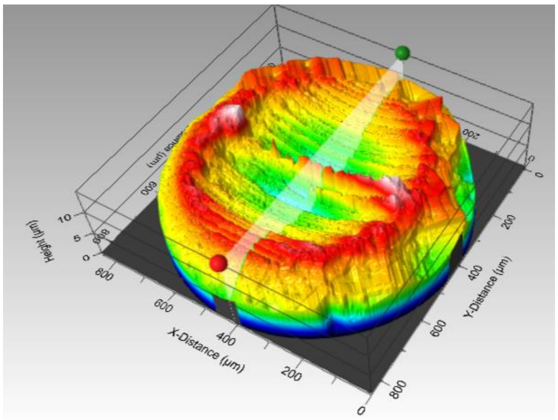

Base Oil + GMO +Soot